RESEARCH MEMORANDUM

EFFECTS OF SPAN AND SPANWISE AND CHORDWISE LOCATION ON THE CONTROL EFFECTIVENESS OF SPOILERS ON A 50° SWEPTBACK WING AT MACH NUMBERS OF 1.41 AND 1.96

By William H. Kindell

Langley Aeronautical Laboratory
Langley Field, Va.

NATIONAL ADVISORY COMMITTEE
FOR AERONAUTICS

WASHINGTON
April 8, 1953

NATIONAL ADVISORY COMMITTEE FOR AERONAUTICS

RESEARCH MEMORANDUM

EFFECTS OF SPAN AND SPANWISE AND CHORDWISE LOCATION ON THE CONTROL EFFECTIVENESS OF SPOILERS ON A 50° SWEPTBACK WING AT MACH NUMBERS OF 1.41 AND 1.96

By William H. Kindell

SUMMARY

An investigation has been made in the Langley 9- by 12-inch supersonic blowdown tunnel to determine the effects of span and spanwise and chordwise location on the control characteristics of spoilers on a 6-percent-thick, 50° sweptback wing of aspect ratio 2.5 and taper ratio 0.625. Tests were made with spoilers of spans ranging from 25 to 75 percent of wing semispan (b/2) located at the 55-, 65-, and 75-percent-wing-chord stations. In addition, tests were made with a $0.75\frac{b}{2}$ - span row of seven spoiler segments located at the 65-percent-wing-chord stations, projected by being rotated out of the wing about axes located along the wing-chord plane, simulating semaphore arms. The investigation was made at Mach numbers of 1.41 and 1.96. Reynolds numbers ranged from 1.6×10^6 to 2.2×10^6.

The results of the investigation indicate that the inboard spoilers located at the rearward chordwise station produce the highest rolling-moment effectiveness. Spoiler effectiveness increased as the span of the inboard $0.25\frac{b}{2}$ - span spoiler was increased to $0.50\frac{b}{2}$ span, but further increase in span to $0.75\frac{b}{2}$ did little to increase spoiler effectiveness, since the outboard $0.25\frac{b}{2}$ - span spoiler produced little effective rolling moment. Compared with a similar spoiler investigation on a related unswept wing, these results show that sweepback decreases the effectiveness of the outboard spoilers and causes less chordwise shift of the center of pressure with rearward spoiler movement.

The semaphore spoilers deflected from 0° to 20° were about equal to plain spoilers of equal exposed area in lift and rolling-moment effectiveness. Above 20° deflection, however, the semaphore spoilers were considerably more effective.

INTRODUCTION

Previous experimental investigations at supersonic speeds have indicated that spoilers may offer some advantages as lateral controls. Comparing this type of control with flap-type controls of equivalent rolling-moment effectiveness, reference 1 suggests the spoiler-type control might cause less wing twisting moment and reference 2 indicates that spoilers produce smaller hinge moments. Experimental information at supersonic speeds on spoiler-type controls, however, is currently limited. Since existing theory is inadequate for predicting spoiler control characteristics, there is a need for systematic experimental information on spoilers at supersonic speeds. In order to provide such information, two related investigations have been carried out in the Langley 9- by 12-inch supersonic blowdown tunnel. The first investigation (ref. 3) dealt with the effects of size and location of spoilers on an unswept wing of aspect ratio 2.5, taper ratio 0.625, and hexagonal 6-percent-thick airfoil sections at a Mach number of 1.9. The second investigation, covered by the present report, is a similar spoiler investigation on a wing of the same aspect ratio, taper ratio, and airfoil section, but having a 45° sweptback midchord line resulting in approximately 50° leading-edge sweepback. It is interesting to note that wings geometrically similar to the two used in the above investigations have been used in several other flap and spoiler investigations (refs. 4 to 7).

In the present investigation, spoilers of spans ranging from 25 to 75 percent of the wing semispan were tested at 55-, 65-, and 75-percent-wing-chord stations. The spoilers were projected up to 6 percent of the local wing chord. In addition, a $0.75\frac{b}{2}$ - span row of semaphore spoilers was tested at the 65-percent-wing-chord station. This row of semaphore spoilers simulated seven equal-length spoilers, 6 percent local wing chord wide, that were projected by being rotated out of the wing about axes located along the wing-chord plane. These spoilers were tested at deflections of 10°, 20°, 45°, and 90° measured in a plane normal to the wing-chord plane.

All tests were made with the wing attached to a half-body. Angle-of-attack limits were -10° and 14°. The tests were made at Mach numbers of 1.41 and 1.96 and at Reynolds numbers ranging from 1.6×10^6 to 2.2×10^6.

COEFFICIENTS AND SYMBOLS

C_L	lift coefficient, $\frac{\text{Lift}}{qS}$
C_D	drag coefficient, $\frac{\text{Drag}}{qS}$
C_m	pitching-moment coefficient, $\frac{\text{Pitching moment about } 0.25\bar{c}}{qS\bar{c}}$
$C_{l_{gross}}$	gross rolling-moment coefficient, $\frac{\text{Wing-panel rolling moment}}{2qSb}$
$C_{n_{gross}}$	gross yawing-moment coefficient, $\frac{\text{Wing-panel yawing moment}}{2qSb}$
C_l	rolling-moment coefficient, $C_{l_{gross}} - C_{l_{gross}(h/c=0)}$
C_n	yawing-moment coefficient, $C_{n_{gross}} - C_{n_{gross}(h/c=0)}$
$\Delta C_L, \Delta C_D, \Delta C_m$	increment in lift, drag, and pitching-moment coefficients due to spoiler projection
q	free-stream dynamic pressure, lb/sq in.
S	semispan wing area, sq in.
S_s	exposed spoiler area, sq in.
c	wing chord, in.
$\bar{c}$	mean aerodynamic chord, in.
b	wing span, twice distance from wing root chord to wing tip, in.
b_s	spoiler span
y_o	spanwise location of outboard end of spoiler
y_s	spanwise location of inboard end of spoiler

h	spoiler projection measured from wing surface normal to wing-chord plane, in.
δ	angle of deflection of semaphore spoiler segments
α	angle of attack, deg
R	Reynolds number based on $\bar{c}$
M	Mach number

MODEL

The geometry of the semispan model tested is shown in figure 1. The wing has a 45° sweptback midchord line, an aspect ratio of 2.5, a taper ratio of 0.625, and has 6-percent-thick hexagonal airfoil sections with streamwise 30-percent-chord wedges forming the leading and trailing edges. The angles between the surfaces of the wedges are 11.42°.

The spoilers (see fig. 1), projected out of the upper surface of a left wing model, were made up of three spoiler segments each of $0.25\frac{b}{2}$ span which were tested separately and in various combinations of inboard, center, and outboard segments at the 55-, 65-, and 75-percent-wing-chord stations, as shown in the following table:

Included spoiler segments	$\frac{b_s}{b/2}$	$\frac{y_s}{b/2}$
Inboard, center, outboard	0.75	0.20
Center, outboard	.50	.45
Inboard, center[a]	.50	.20
Outboard	.25	.70
Inboard[a]	.25	.20
Center[a]	.25	.45

[a]Not tested at the 0.55c location.

Spoiler projection was varied from 0 to 6 percent of local wing chord except at the 75-percent-chord station, where this projection would have exceeded the local wing thickness. At this location, the maximum spoiler projection was 4 percent of the local wing chord. The top of each spoiler was beveled, as shown in figure 1, to present a sharp edge to the air stream.

In addition, tests were made with a $0.75\frac{b}{2}$ - span row of semaphore spoilers (see fig. 2) located at the 65-percent-wing-chord station. The spanwise length of each of the seven spoilers in the row was 10 percent of the wing semispan and the width was 6 percent of the local wing chord, the thickness of the wing. When projected, the spoilers simulate semaphore arms rotated out of the wing about axes located along the wing-chord plane and 3 percent of local wing chord (half the wing thickness) from the inboard end of the individual spoilers. The projected height of the spoilers above the wing-chord plane increased from the inboard to the outboard spoiler, since the over-all length of each spoiler remained the same while the wing thickness decreased. The spoilers were tested at angles of deflection of 10°, 20°, 45°, and 90° measured with respect to the wing-chord plane.

TUNNEL AND TEST TECHNIQUE

The tests were conducted in the Langley 9- by 12-inch supersonic blowdown tunnel. This tunnel is of the nonreturn type utilizing exhaust air from the Langley 19-foot pressure tunnel. Air enters the tunnel at an absolute pressure of from 2 to $2\frac{1}{3}$ atmospheres. Heating and drying units condition the entering air to insure condensation-free flow in the test section. The criteria for the amount of heating and drying necessary were obtained from reference 8. The two test-section Mach numbers are provided by interchangeable nozzle blocks. The free-stream Mach numbers of these blocks have been calibrated at 1.41 ±0.02 and 1.96 ±0.02. The variations in stream angle in the vicinity of the test section occupied by the model is for the tunnel-clear condition $\pm 0.25^\circ$ at $M = 1.41$ and $\pm 0.20^\circ$ at $M = 1.96$. The mean flow, as determined from these variations, is approximately parallel to the tunnel axis. A more extensive description of the flow conditions in the test section of each nozzle block may be found in reference 9.

The semispan model was cantilevered from a strain-gage balance mounted flush with the tunnel floor which was free to rotate through the angle-of-attack range. A half-body of revolution was fixed to the wing. A 0.25-inch shim was attached to the half-body to raise it off the tunnel floor and thus minimize the effects of the tunnel-floor boundary layer on the flow over its surface. A description of the development of this shim is given in reference 10. A gap of about 0.010 inch was maintained between the test body and the tunnel floor.

ACCURACY

The magnitudes of errors in coefficient resulting from general considerations of balance calibration accuracy, repeatability of the data, and accuracy of measurements are believed to be about as follows:

C_L	±0.005
C_l	±0.001
C_D	±0.001
C_m	±0.002
C_n	±0.0002

The angle-of-attack values relative to the tunnel axis are believed to be accurate within ±0.05°, based upon limitations of the mechanical angle-of-attack system and the calibration charts from which the actual values were obtained. Possible errors in C_D and C_n increase to some extent from that indicated in the table with increases in angle of attack. The ability to determine trends from the data is believed to be somewhat better than indicated in the table because the relative accuracy of one coefficient with respect to another is not influenced by errors in balance calibration, and the repeatability of the data is in general better than indicated in the table.

RESULTS AND DISCUSSION

Representative basic data for the various wing-spoiler combinations tested are presented in figures 3 to 7. Incremental aerodynamic coefficients due to spoiler projection, obtained from the basic data plots, are presented in figures 8 to 12 for three representative angles of attack. In these plots, the data for spoilers projected from the lower surface were obtained by proper sign reversal of the negative angle-of-attack data. This was possible since the model tested was symmetrical about the wing-chord plane.

The summary plots of figures 8 to 12 show that for most configurations nonlinear variations of coefficient with spoiler projection exists, and reversals in rolling moment, lift increment, and pitching moment occur for some spoilers projected from the lower surface. These figures also indicate that a decrease in coefficient occurs with an increase in Mach number. To illustrate better the effects of spoiler chordwise position, additional plots of aerodynamic coefficient versus chordwise location for the representative spoiler projection of 0.04c are presented in figures 13 to 17.

In figures 8 to 12, the curves for the $0.25\frac{b}{2}$ - span and $0.50\frac{b}{2}$ - span outboard spoilers located at the 0.55c station are defined by just two points, since data were obtained for only the projection $h/c = 0.06$ of these spoilers. Consequently, the data in figures 13 to 17 for these two spoilers projected 0.04c from the 0.55c location were obtained by interpolation.

Rolling-Moment and Lift Characteristics

Effects of chordwise location.- Generally the data of figures 13 and 14 show increases in rolling moment and lift increment with rearward spoiler movement for spoilers projected from the upper and lower surfaces. This trend was indicated in reference 3 for similar spoilers on an unswept wing having airfoil sections, aspect ratio, and taper ratio identical to the wing in this report. Continuation of this trend with further rearward spoiler movement is indicated in reference 11 which compares spoilers located at the 0.70-chord line with trailing-edge spoilers on two, untapered full-blunt trailing-edge wings of aspect ratio 2.7 with 0° and 45° sweepback.

The amount of increase in effectiveness with rearward chordwise movement appears to increase with angle of attack for the lower-surface spoilers and to decrease with angle of attack for the upper-surface spoilers (fig. 13). These decreases with angle of attack for the upper-surface spoilers are such that for some spoilers there is no increase in effectiveness with rearward chordwise movement at high angles of attack. The effects of angle of attack for the lower-surface spoilers are generally less at the 0.65c and 0.75c stations than at the 0.55c location.

The increase in rolling moment and lift increment with rearward movement of the $0.50\frac{b}{2}$ - span and $0.75\frac{b}{2}$ - span spoiler is generally greater between the 0.55c and 0.65c locations than between the 0.65c and 0.75c locations (figs. 13 and 14). This is particularly pronounced in the case of rolling moment at $M = 1.41$ (fig. 13(a)). The lower rate of increase in spoiler effectiveness between the 0.65c and 0.75c locations may be explained by referring to the cross-sectional view of the airfoil-spoiler combination in figure 1. The spoilers located at the 0.55c and 0.65c stations are projected from the flat 40-percent midsection of the airfoil, while the spoilers located at the 0.75c station extend outward from the trailing-edge wedge section. Thus, for equal spoiler projections, the spoilers located at the 0.75c station do not project as far above the level of the flat midsection of the airfoil as do the spoilers located at the 0.55c and 0.65c stations. Therefore, the wing area affected by the compression region ahead of the spoiler at the 0.75c station might be expected to be smaller, resulting in less negative lift,

than if the spoiler height above the flat midsection of the airfoil had been the same as for the spoilers at the 0.55c and 0.65c stations. An exception to the generally lower rate of increase in effectiveness with rearward movement of the spoilers from the 0.65c station is indicated for the $0.50\frac{b}{2}$ - span and $0.75\frac{b}{2}$ - span spoilers at an angle of attack of 10° and a Mach number of 1.96 (fig. 13(b)).

Figures 13 and 14 show the increases in effectiveness with rearward movement from 0.65c to 0.75c of the $0.25\frac{b}{2}$ - span spoilers to be approximately equal for the three spanwise locations, except for rolling moment at $M = 1.41$ (fig. 13(a)), where the effectiveness of the center $0.25\frac{b}{2}$ - span spoiler increased more sharply with rearward movement than either the outboard or inboard segments. Although this trend of the center $0.25\frac{b}{2}$ - span spoiler appears inconsistent with the pattern set by the outboard and inboard $0.25\frac{b}{2}$ - span spoilers, the same effect was obtained by the spoilers projected $h/c = 0.02$ (fig. 8(a)). The reason for this effect is not known. Since the lift-coefficient variations are similar for the three spanwise locations at $M = 1.41$, however, this trend indicates an outboard shift in the center of loading with the rearward movement of the center $0.25\frac{b}{2}$ - span spoilers from the flat center panel of the wing to the trailing-edge wedge.

Effects of spanwise location.- The data of figures 13 and 14 show the inboard spanwise location to be the most effective for the partial-span spoilers. This trend was indicated in reference 1 for a wing with 60° quarter-chord-line sweepback and taper ratio 0.6. A possible explanation for the greater lift effectiveness of the inboard spoiler would appear to be that the effect of the fuselage in restricting the flow from the compression region ahead of this spoiler to the expansion region behind the spoiler causes a weaker expansion behind the spoiler with a resulting increase in lift increment. Comparisons of the amounts by which the rolling moment and lift increase as the spoilers move inboard indicate that the location of the center of loading due to spoiler deflection does not move inboard in proportion to spoiler movement. For instance, in the case of the $0.50\frac{b}{2}$ - span spoilers, movement from the $0.45\frac{b}{2}$ to the $0.20\frac{b}{2}$ location results in proportional increases in incremental lift and rolling moment which are about equal while the distance from the roll axis to the center of spoiler decreases 36 percent. Similar trends may be noted in some cases for the $0.25\frac{b}{2}$ - span spoilers.

The data of figures 13 and 14 show that the effectiveness of the center $0.25\frac{b}{2}$ - span spoilers generally was between that for the inboard and that for the outboard $0.25\frac{b}{2}$ - span spoilers. The outboard $0.25\frac{b}{2}$ - span spoiler had very little effective rolling moment and lift, and when projected from the lower surface of the wing it produced reversals at angles of attack of 4° and above.

Effects of spoiler span.- Figure 18 is a representative plot of rolling moment and incremental lift against location of the outboard end of the spoiler for $\alpha = 4^\circ$ and $h/c = 0.04$ at $M = 1.41$ and 1.96. The data of this figure show that increasing the span of the $0.25\frac{b}{2}$ - span inboard spoiler by the addition of the center $0.25\frac{b}{2}$ - span spoiler generally produced results near the sum of the results of these two spoilers tested separately. This is particularly evident at the 0.55c location where variation of rolling moment and lift increment with span is nearly linear and curves for the $\frac{y_s}{b/2} = 0.20$ and 0.45 spoilers are parallel. Increasing the span of the inboard $0.50\frac{b}{2}$ - span spoilers located at the 0.65c and 0.75c line to $0.75\frac{b}{2}$ span did little to increase spoiler effectiveness even though this addition increases spoiler span 50 percent. Further indications of the low effectiveness of the outboard $0.25\frac{b}{2}$ - span spoiler segments is illustrated by the fact that the outboard $0.50\frac{b}{2}$ - span spoiler was roughly half as effective as the $0.75\frac{b}{2}$ - span spoiler, while the inboard $0.50\frac{b}{2}$ - span spoiler was in many cases equal in rolling-moment and lift effectiveness to the $0.75\frac{b}{2}$ - span spoiler (fig. 18). A possible cause for the poor effectiveness of the outboard spoilers could be losses in spoiler-induced loading due to flow over the tip of the wing. Reference 3, a similar spoiler investigation on an unswept wing of aspect ratio 2.5 and taper ratio 0.625, shows that spoiler effectiveness was little affected by moving the spoilers inboard. This result indicates that the large difference in effectiveness between the outboard and inboard spoilers of the present report is a sweep effect.

In reference 1, it is pointed out that the addition of simulated actuating arms to the spoiler ailerons of a wing with 60° quarter-chord-line sweepback, aspect ratio 2, and taper ratio 0.6 produced increases in rolling effectiveness, particularly at angles of attack of 4° and above. These actuating arms were small triangular-shaped pieces of

sheet metal located adjacent and normal to the spoiler and wing at equal intervals along the spoiler length. Apparently the actuating arms acted as fences in restricting the spanwise flow along the front of the spoiler. The addition, then, of fences at the ends and along the spoilers might be expected to result in a similar increase in the effectiveness of the spoilers of the present investigation.

Pitching-Moment Characteristics

The data of figure 15 show that the incremental pitching-moment coefficients increase for the spoilers projected from the upper surface and decrease for the spoilers projected from the lower surface as the spoiler chordwise location moves rearward. The amount of variation in incremental pitching moment with the rearward chordwise movement of the spoiler location generally decreases with an increase in angle of attack for the positive projected spoilers and remains about the same or increases with increase in angle of attack for the negative projected spoilers. These trends reflect those of wing loading previously discussed in the section of this report entitled "Rolling-Moment and Lift Characteristics." Comparing these results with those of reference 3, a similar spoiler investigation on a related unswept wing, shows that the unswept condition produced much larger changes in pitching moment in proportion to the increase in lift increment with rearward spoiler movement, indicating there is a greater chordwise shift of the center of pressure with rearward spoiler movement for the unswept condition than for the swept condition.

At 0° angle of attack, the data of figure 15 show reversals in pitching moment for the spoilers located ahead of about the 0.60c or 0.65c station. These reversals disappear for the spoilers projected from the upper surface with an increase in angle of attack, but they remain throughout the angle-of-attack range for the spoilers projected from the lower surface. In fact, the chordwise location ahead of which these reversals occur for the lower-surface spoilers appears to move rearward with increases in angle of attack above 4°.

It is worthy of note that the pitching moments produced by the spoilers tested for this report are considerably less than those produced by flap-type controls of reference 7 at equal rolling moments. For example, the $0.75\frac{b}{2}$ - span spoiler located at the 0.75c position (where the maximum pitching-moment increment for the spoilers tested was produced) and projected 0.04c at 0° angle of attack produces a pitching-moment increment at $M = 1.96$, figure 15(b), that is about 75 percent of the pitching-moment increment produced by the $0.75\frac{b}{2}$ - span, 0.25-chord flap of reference 7, deflected 6° to give equal rolling-moment effectiveness. This comparison indicates that the wing twisting

moment produced by spoilers would probably be less than for flap-type controls.

Drag and Yawing-Moment Characteristics

In general, the data of figures 16 and 17 show a decrease in the absolute values of incremental drag and yawing moment for the positive projected spoilers, and an increase in these values for most negative projected spoilers with an increase in angle of attack. The positive projected spoilers at low angles of attack and the negative projected spoilers throughout the angle-of-attack range appear to produce the most drag when located at about the 0.65-chord station. This result was noted in reference 3 for spoilers located on a related unswept wing. The decrease in drag and yawing moment going from the 0.65c to the 0.75c station in these cases might be associated with the decreasing frontal area resulting from movement of the spoiler from the flat mid-section of the airfoil to the trailing-edge wedge.

The inboard partial-span spoilers produce more drag than either the outboard or midspan spoilers of comparable span, as might be expected from the consideration of the lift loading characteristics, previously discussed, and from the greater absolute projection of the inboard spoilers. It is interesting to note, however, that this larger drag of the inboard spoilers causes less yawing moment than that resulting from the outboard and midspan spoilers, since the differences in moment arm more than compensate for the differences in spoiler drag.

Comparison of Plain and Semaphore Spoilers

The data for the $0.75\frac{b}{2}$ - span row of semaphore spoilers located on the 0.65c station are compared with the data for the similarly located $0.75\frac{b}{2}$ - span plain spoiler in figures 19 to 23. Incremental aerodynamic coefficients for each control due to control deflection are plotted against the ratio of spoiler projected area to half-wing area S_s/S.

The data of figures 19 and 20 show that the row of semaphore spoilers is considerably more effective in lift and rolling moment when deflected above 20° than the plain spoilers of equivalent exposed area (S_s/S of 0.019). Apparently the greater projected height of the semaphore spoilers above 20° deflection, compared with the plain spoiler of equal exposed area, produces an increase in lift loading on the wing that more than compensates for the loading losses caused by flow between the semaphore spoiler units. Below 20° spoiler deflection, the row of

semaphore spoilers and the plain spoilers of equal exposed area are more nearly equal in lift-increment and rolling-moment effectiveness.

Pitching moments produced by the row of semaphore spoilers at higher projections (fig. 21) are generally greater than those produced by plain spoilers of equal exposed area as might be expected from the lift and rolling-moment results. It is interesting to note that, at an angle of attack of 8° and $M = 1.96$, the plain spoilers projected from the lower surface produced reversals in pitching moment, while the lower-surface semaphore spoilers produced an increasing pitching moment.

The higher projections of semaphore spoilers produce drag and yawing moments that are about half again as large at 0° angle of attack as those produced by the plain spoilers of equal exposed area (figs. 22 and 23). This proportion increases with angle of attack for upper-surface projections until it is greater than 2:1 at an angle of attack of 8°. The semaphore spoilers projected from the lower surface produce values of drag and yawing moment between about one-third and one-half greater than those produced by similarly projected plain spoilers of equal exposed area.

CONCLUDING REMARKS

An investigation has been made to determine the effects of span and spanwise and chordwise location on the control characteristics of spoilers on a 50° sweptback wing at Mach numbers of 1.41 and 1.96. Tests were made with various spans and projections of spoilers located at the 55-, 65-, and 75-percent-wing-chord stations. In addition, tests were made with a row of semaphore spoilers located at the 0.65-chord station and comprising 75 percent of the wing semispan ($b/2$).

The results of the investigation indicate that lift and rolling-moment effectiveness increased with rearward chordwise movement of the spoilers and were higher for inboard than for midspan or outboard spoilers. Lift and rolling-moment effectiveness increased when the span of the inboard spoiler was increased from $0.25\frac{b}{2}$ to $0.50\frac{b}{2}$, but the addition of the outboard $0.25\frac{b}{2}$ - span spoiler segment did little to increase the effectiveness of any of the spoilers. The outboard $0.25\frac{b}{2}$ - span spoiler projected from the lower surface of the wing produced lift and rolling-moment reversals under certain conditions at all three chordwise locations. Compared with a similar spoiler investigation on a related

unswept wing, these results show that sweepback decreases the effectiveness of the outboard spoilers and causes less chordwise shift of the center of pressure with rearward spoiler movement.

The lift and rolling-moment effectiveness produced by semaphore spoilers deflected from 0° to 20° about equaled that of plain spoilers of equal exposed area. Above 20° deflection, however, the semaphore spoilers were considerably more effective. The drag of the semaphore spoilers varied from about one and one-third to two times the drag produced by plain spoilers of equal exposed area.

Langley Aeronautical Laboratory,
National Advisory Committee for Aeronautics,
Langley Field, Va.

REFERENCES

1. Hammond, Alexander D.: Lateral-Control Investigation of Flap-Type and Spoiler-Type Controls on a Wing With Quarter-Chord-Line Sweepback of 60°, Aspect Ratio 2, Taper Ratio 0.6, and NACA 65A006 Airfoil Section. Transonic-Bump Method. NACA RM L50E09, 1950.

2. Fikes, Joseph E.: Hinge-Moment and Other Aerodynamic Characteristics at Transonic Speeds of a Quarter-Span Spoiler on a Tapered 45° Sweptback Wing of Aspect Ratio 3. NACA RM L52A03, 1952.

3. Conner, D. William, and Mitchell, Meade H., Jr.: Effects of Spoiler on Airfoil Pressure Distribution and Effects of Size and Location of Spoilers on the Aerodynamic Characteristics of a Tapered Unswept Wing of Aspect Ratio 2.5 at a Mach Number of 1.90. NACA RM L50I20, 1951.

4. Strass, H. Kurt: Additional Free-Flight Tests of the Rolling Effectiveness of Several Wing-Spoiler Arrangements at High Subsonic, Transonic, and Supersonic Speeds. NACA RM L8I23, 1948.

5. Vogler, Raymond D., Lockwood, Vernard E., and Turner, Thomas R.: An Investigation at Transonic Speeds of the Effects of Control Chord and Span on the Control Characteristics of a Tapered Wedge-Type Wing of Aspect Ratio 2.5. Transonic-Bump Method. NACA RM L51G03, 1951.

6. Mitchell, Meade H., Jr.: Effects of Varying the Size and Location of Trailing-Edge Flap-Type Controls on the Aerodynamic Characteristics of an Unswept Wing at a Mach Number of 1.90. NACA RM L50F08, 1950.

7. Jacobsen, Carl R.: Effects on Control Effectiveness of Systematically Varying the Size and Location of Trailing-Edge Flaps on a 45° Sweptback Wing at a Mach Number of 1.9. NACA RM L51I26, 1951.

8. Burgess, Warren C., Jr., and Seashore, Ferris L.: Criterions for Condensation-Free Flow in Supersonic Tunnels. NACA TN 2518, 1951.

9. May, Ellery B., Jr.: Investigation of the Effects of Leading-Edge Chord-Extensions on the Aerodynamic and Control Characteristics of Two Sweptback Wings at Mach Numbers of 1.41, 1.62, and 1.96. NACA RM L50L06a, 1951.

10. Conner, D. William: Aerodynamic Characteristics of Two All-Movable Wings Tested in the Presence of a Fuselage at a Mach Number of 1.9. NACA RM L8H04, 1948.

11. Jacobsen, Carl R.: Control Characteristics of Trailing-Edge Spoilers on Untapered Blunt Trailing-Edge Wings of Aspect Ratio 2.7 With 0° and 45° Sweepback at Mach Numbers of 1.41 and 1.96. NACA RM L52J28, 1952.

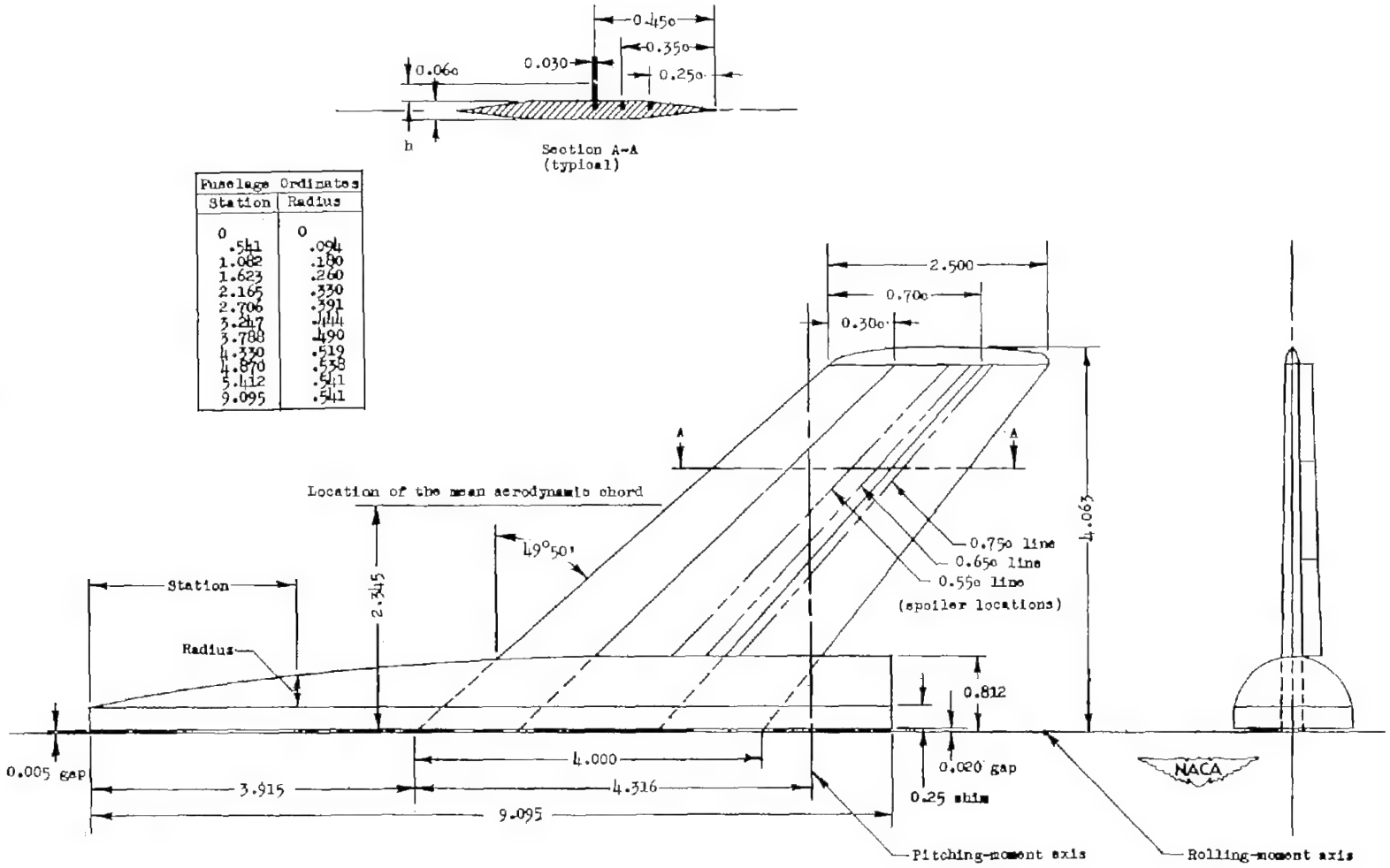

Figure 1.- Details of semispan left wing model, spoiler locations, and typical $0.75\frac{b}{2}$ - span spoiler. All dimensions in inches.

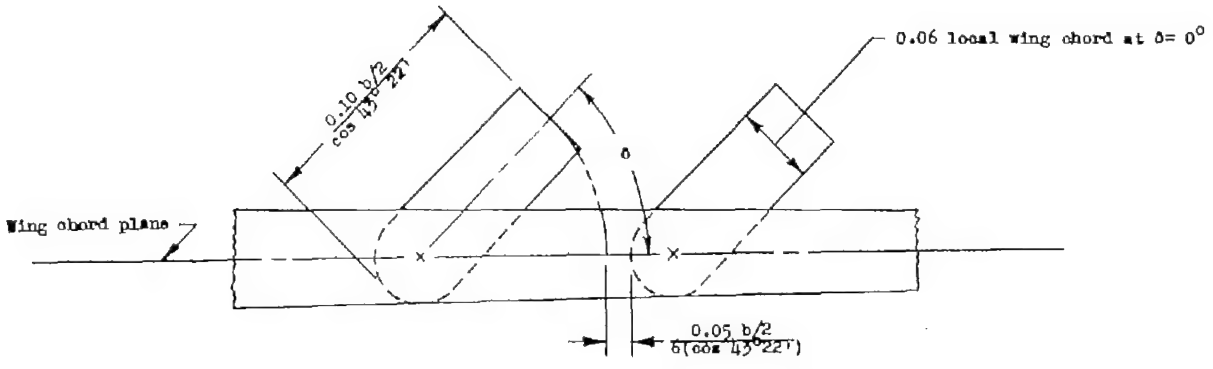

Projection of typical semaphore spoilers on plane through 0.65c station

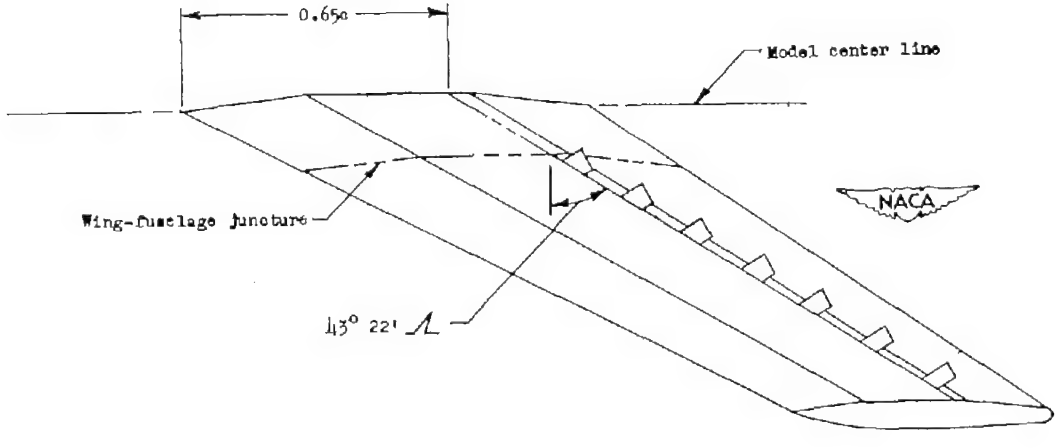

Figure 2.- Details of $0.75\frac{b}{2}$ - span row of semaphore spoilers located on the 0.65c station.

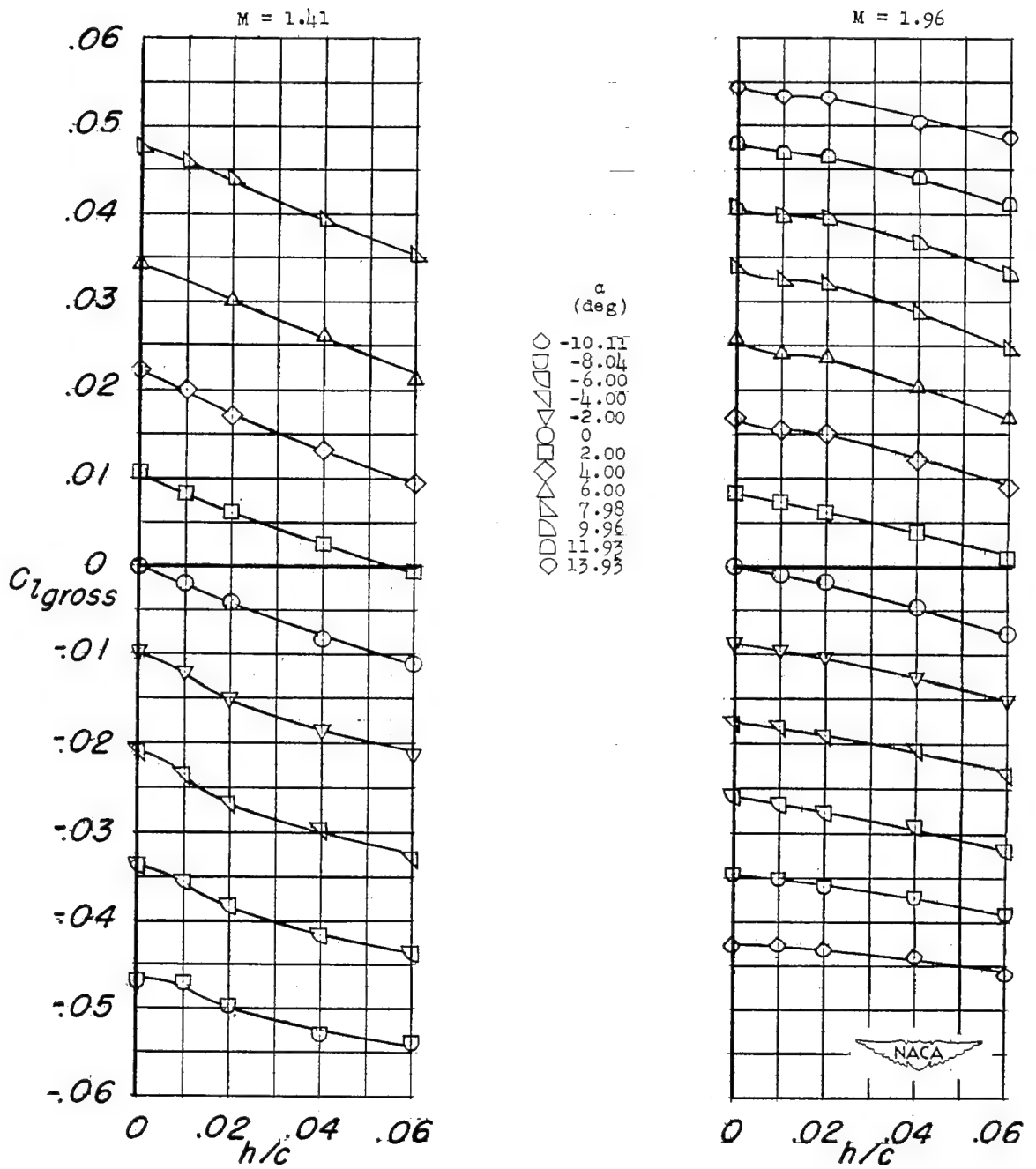

(a) $b_s = 0.75\frac{b}{2}$; $y_s = 0.20\frac{b}{2}$.

Figure 3.- Rolling-moment characteristics of a swept semispan wing equipped with plain spoilers located on the 0.65c station.

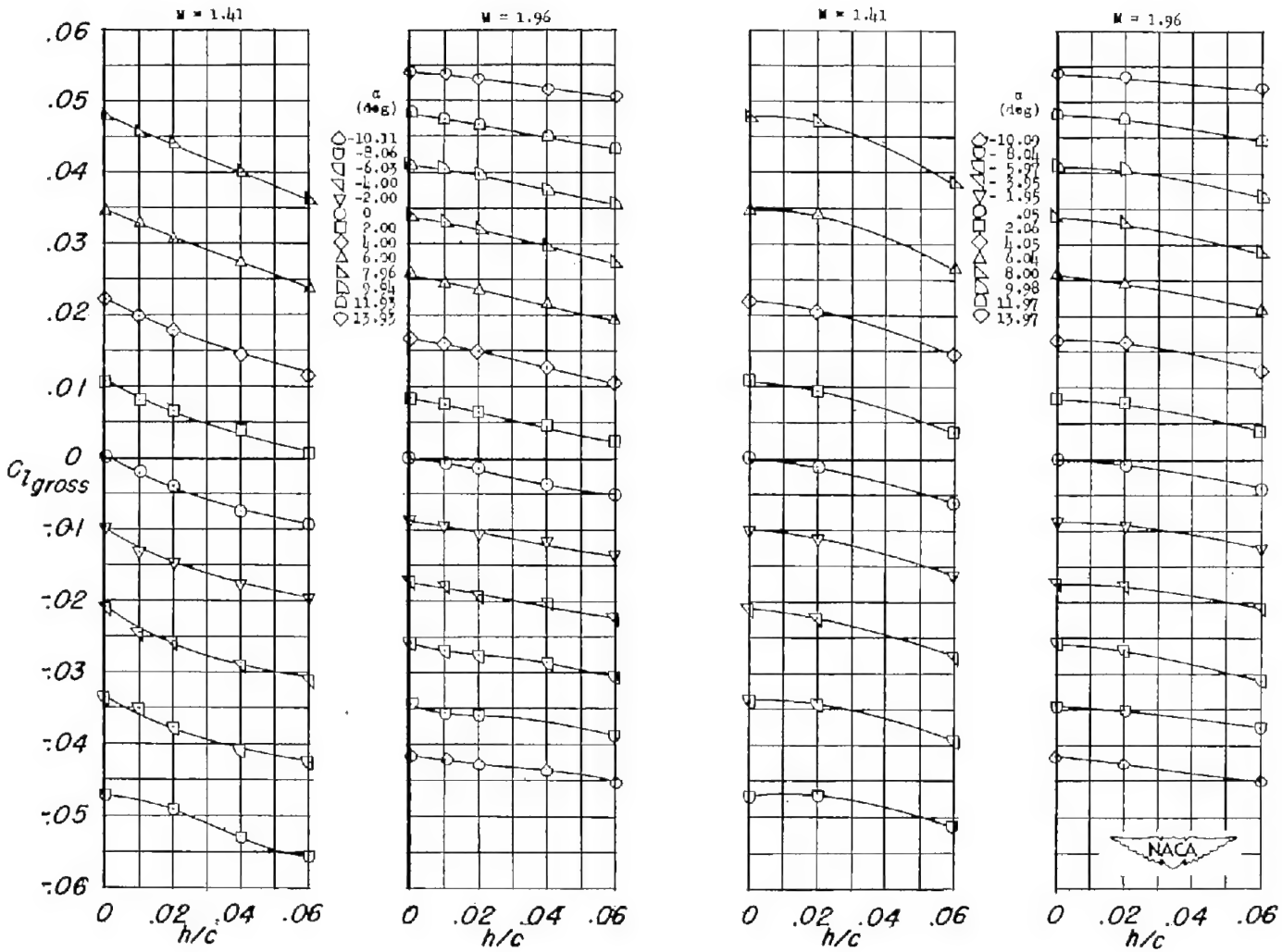

(b) $b_S = 0.50\frac{b}{2}$; $y_S = 0.20\frac{b}{2}$.

(c) $b_S = 0.25\frac{b}{2}$; $y_S = 0.20\frac{b}{2}$.

Figure 3.- Concluded.

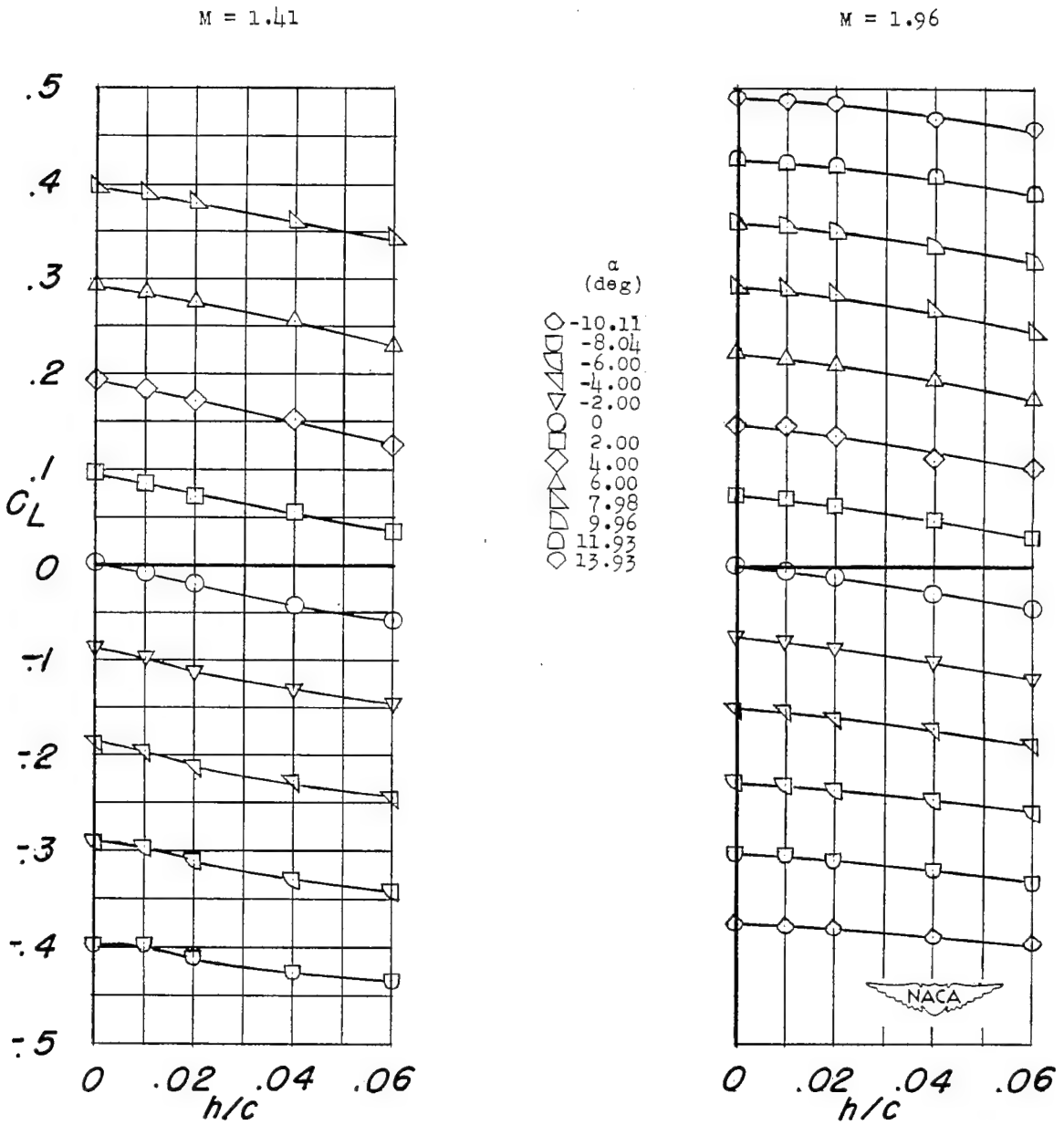

(a) $b_s = 0.75\frac{b}{2}$; $y_s = 0.20\frac{b}{2}$.

Figure 4.- Lift characteristics of a swept semispan wing equipped with plain spoilers located on the 0.65c station.

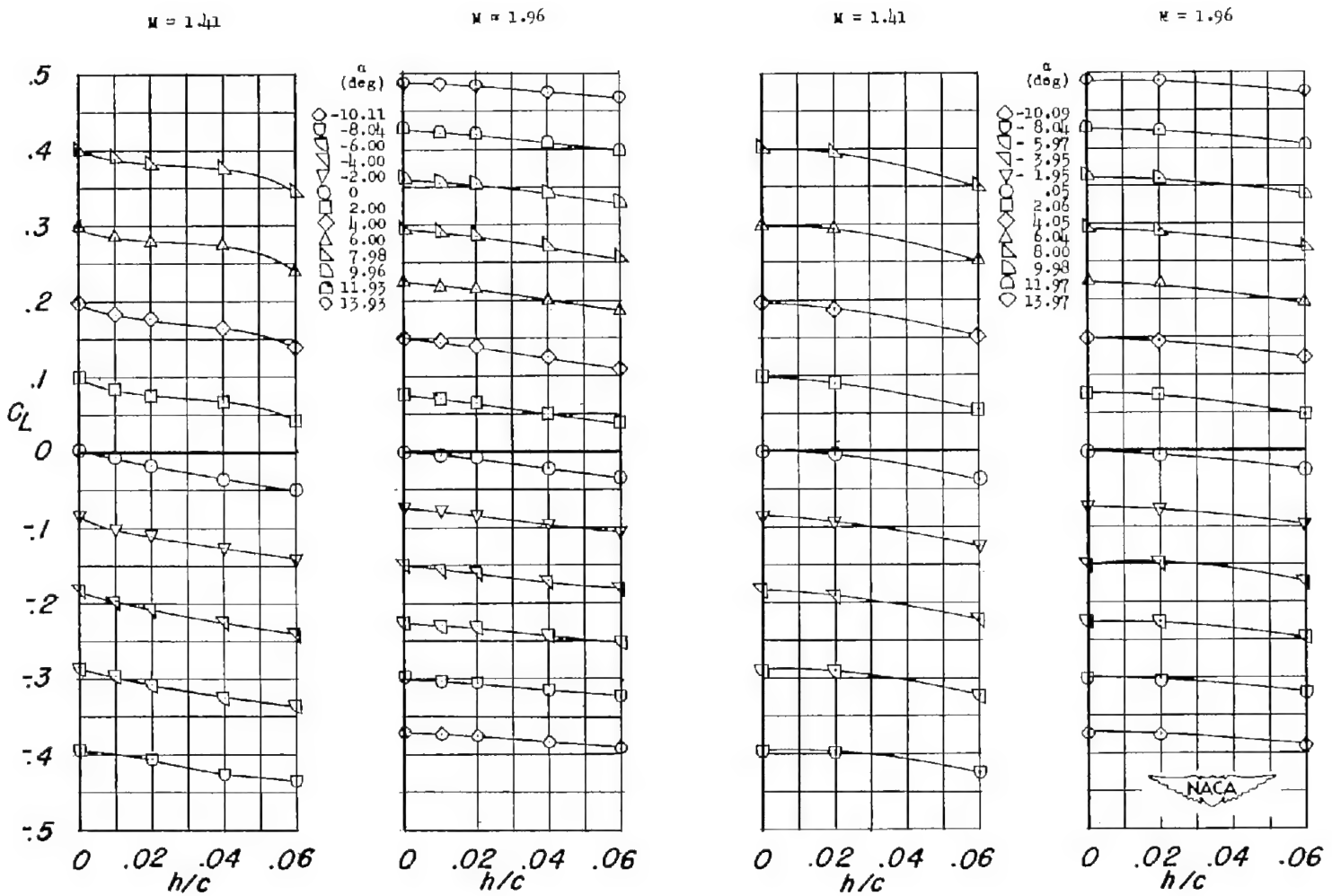

(b) $b_S = 0.50\frac{b}{2}$; $y_S = 0.20\frac{b}{2}$.

(c) $b_S = 0.25\frac{b}{2}$; $y_S = 0.20\frac{b}{2}$.

Figure 4.- Concluded.

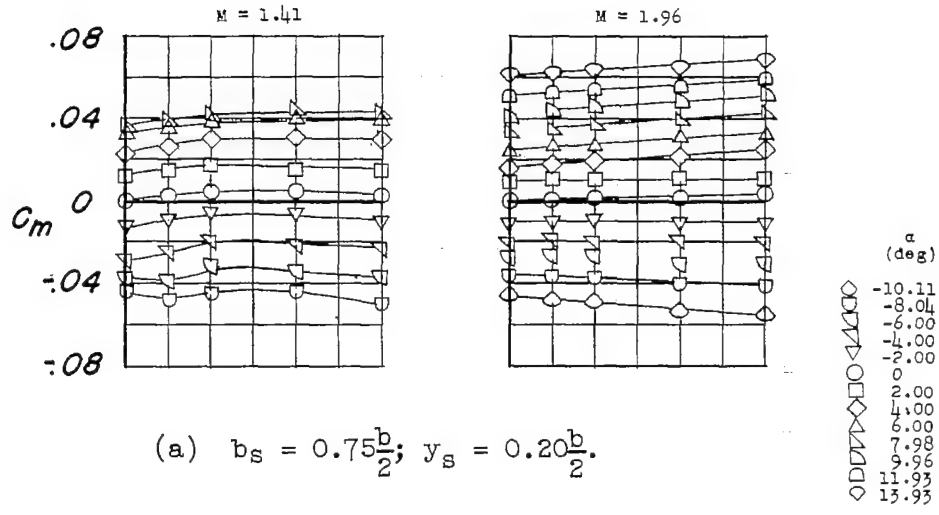

(a) $b_s = 0.75\frac{b}{2}$; $y_s = 0.20\frac{b}{2}$.

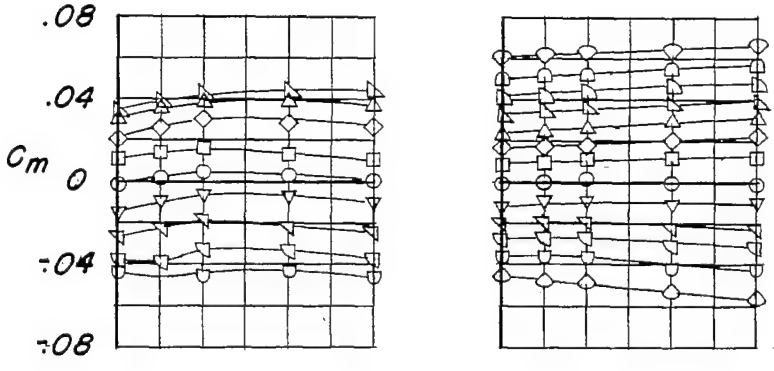

(b) $b_s = 0.50\frac{b}{2}$; $y_s = 0.20\frac{b}{2}$.

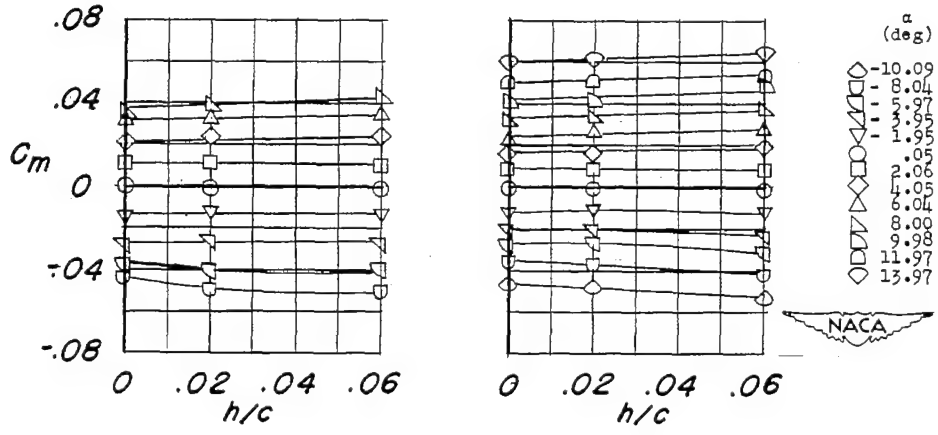

(c) $b_s = 0.25\frac{b}{2}$; $y_s = 0.20\frac{b}{2}$.

Figure 5.- Pitching-moment characteristics of a swept semispan wing equipped with plain spoilers located on the 0.65c station.

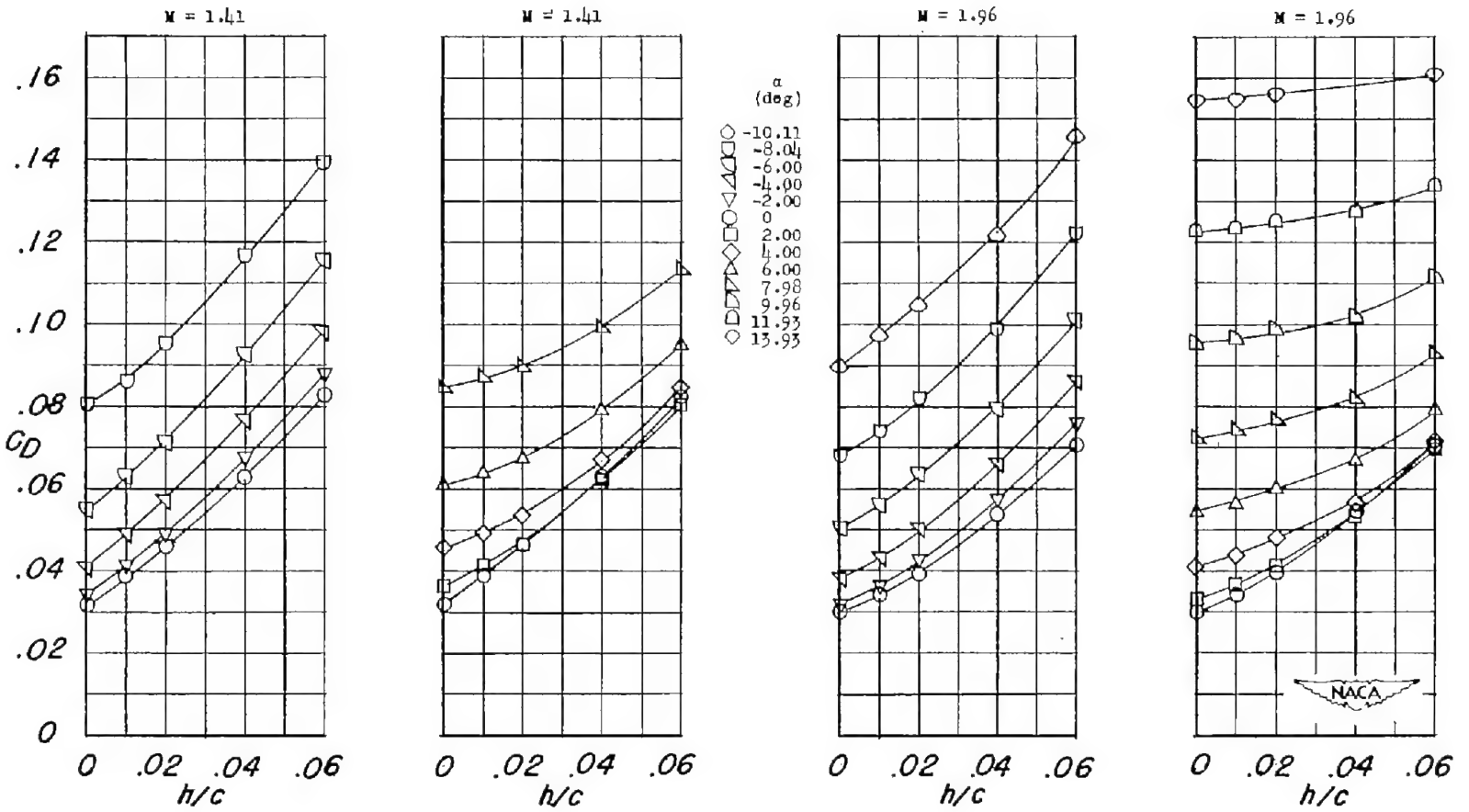

(a) $b_s = 0.75\frac{b}{2}$; $y_s = 0.20\frac{b}{2}$.

Figure 6.- Drag characteristics of a swept semispan wing equipped with plain spoilers located on the 0.65c station.

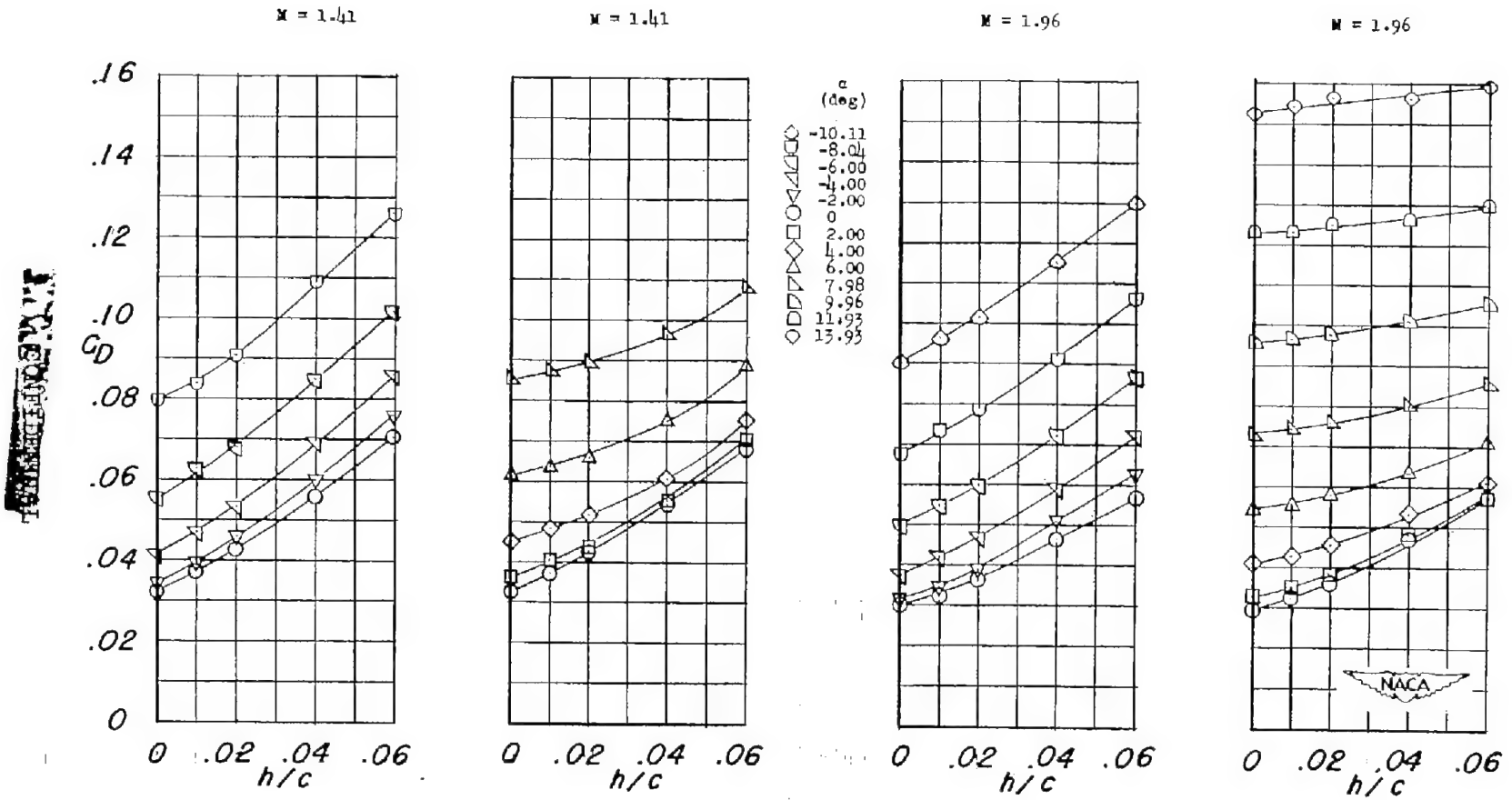

(b) $b_S = 0.50\frac{b}{2}$; $y_S = 0.20\frac{b}{2}$.

Figure 6.- Continued.

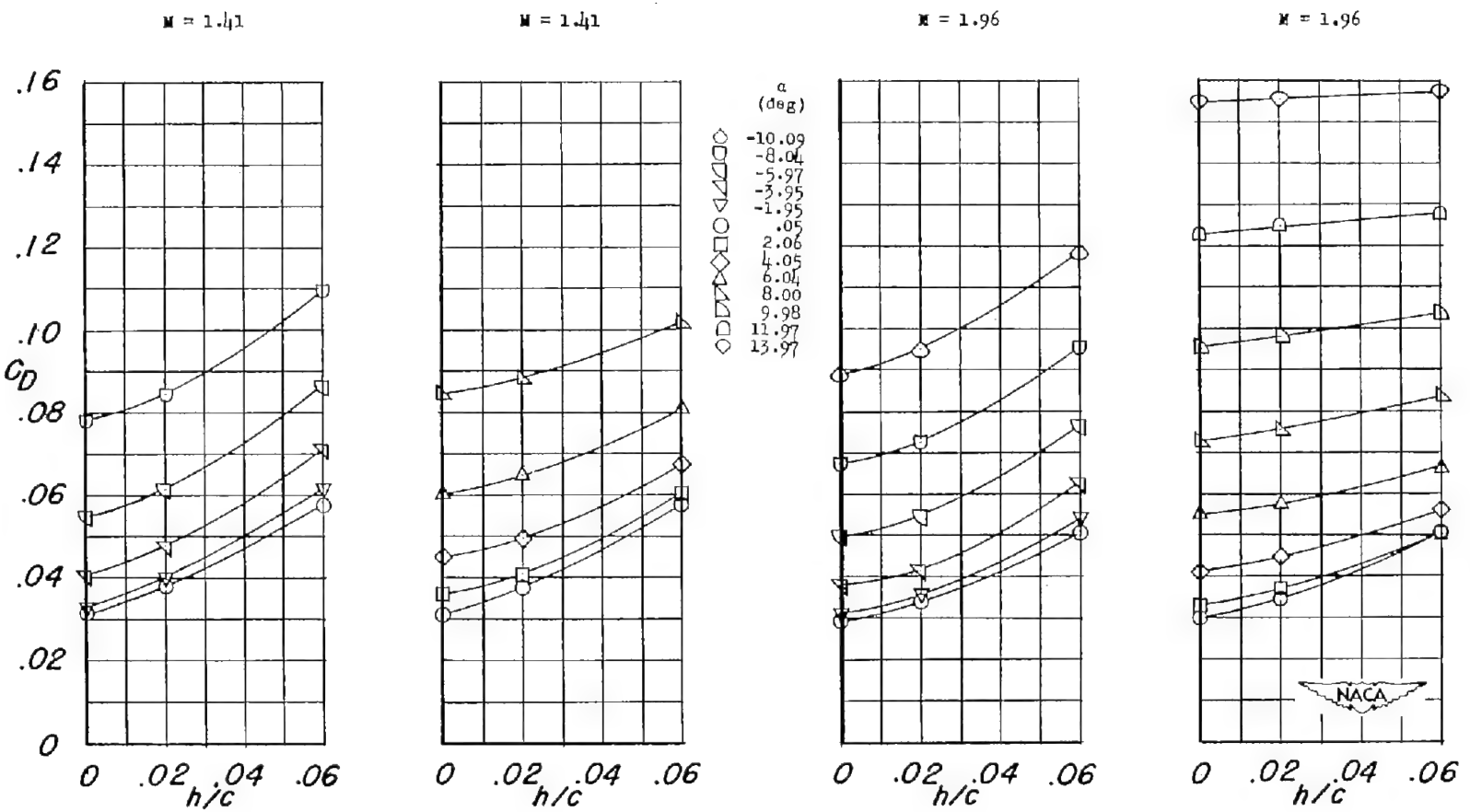

(c) $b_s = 0.25\frac{b}{2}$; $y_s = 0.20\frac{b}{2}$.

Figure 6.- Concluded.

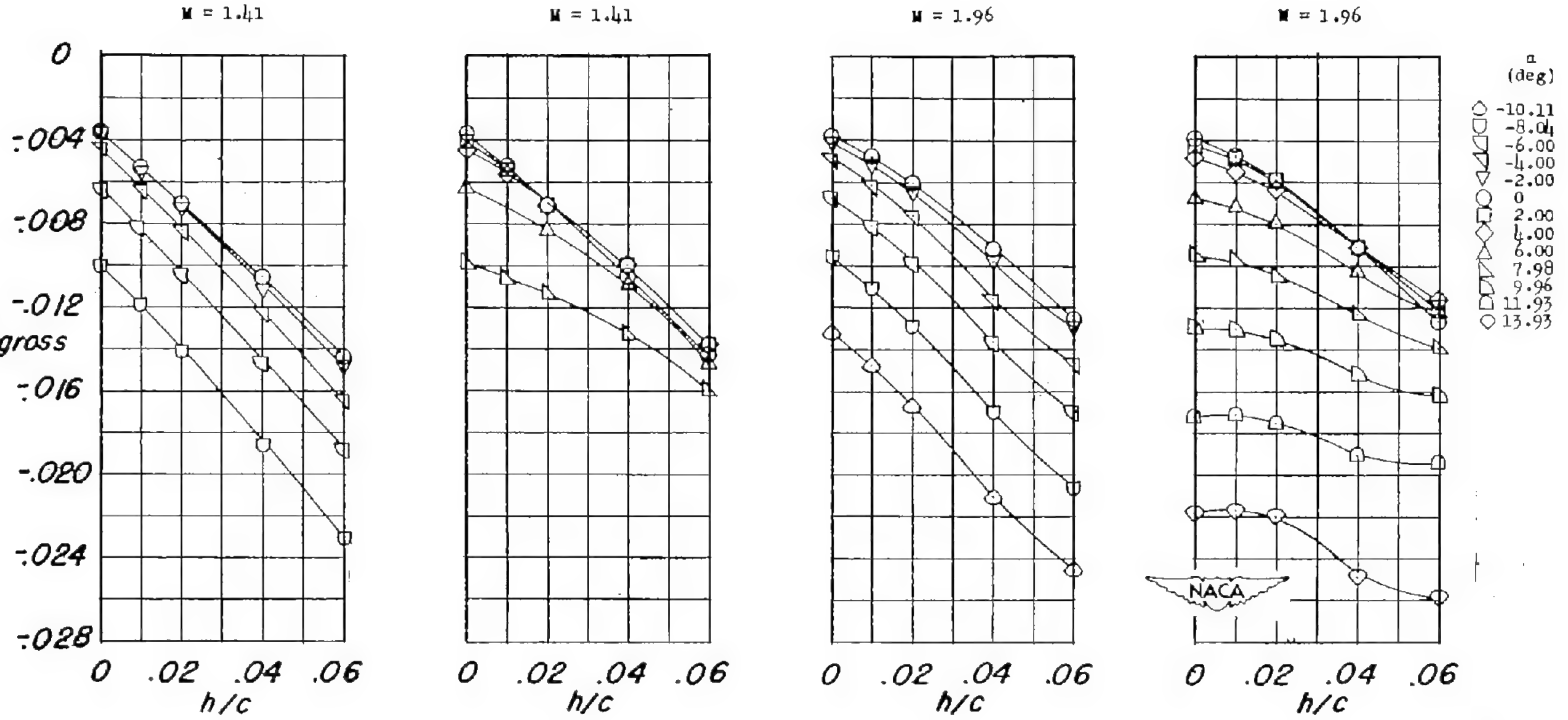

(a) $b_S = 0.75\frac{b}{2}$; $y_S = 0.20\frac{b}{2}$.

Figure 7.- Yawing-moment characteristics of a swept semispan wing equipped with plain spoilers located on the 0.65c station.

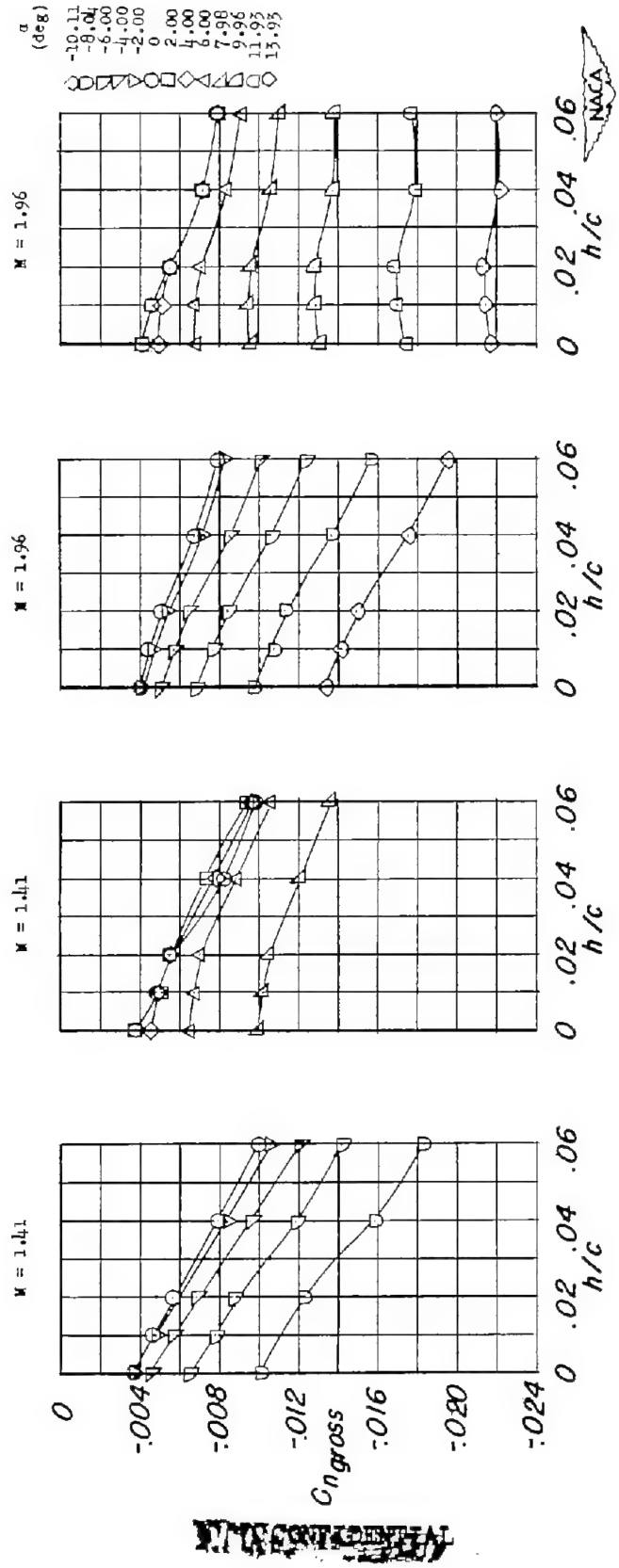

(b) $b_s = 0.50\frac{b}{2}$; $y_s = 0.20\frac{b}{2}$.

Figure 7.- Continued.

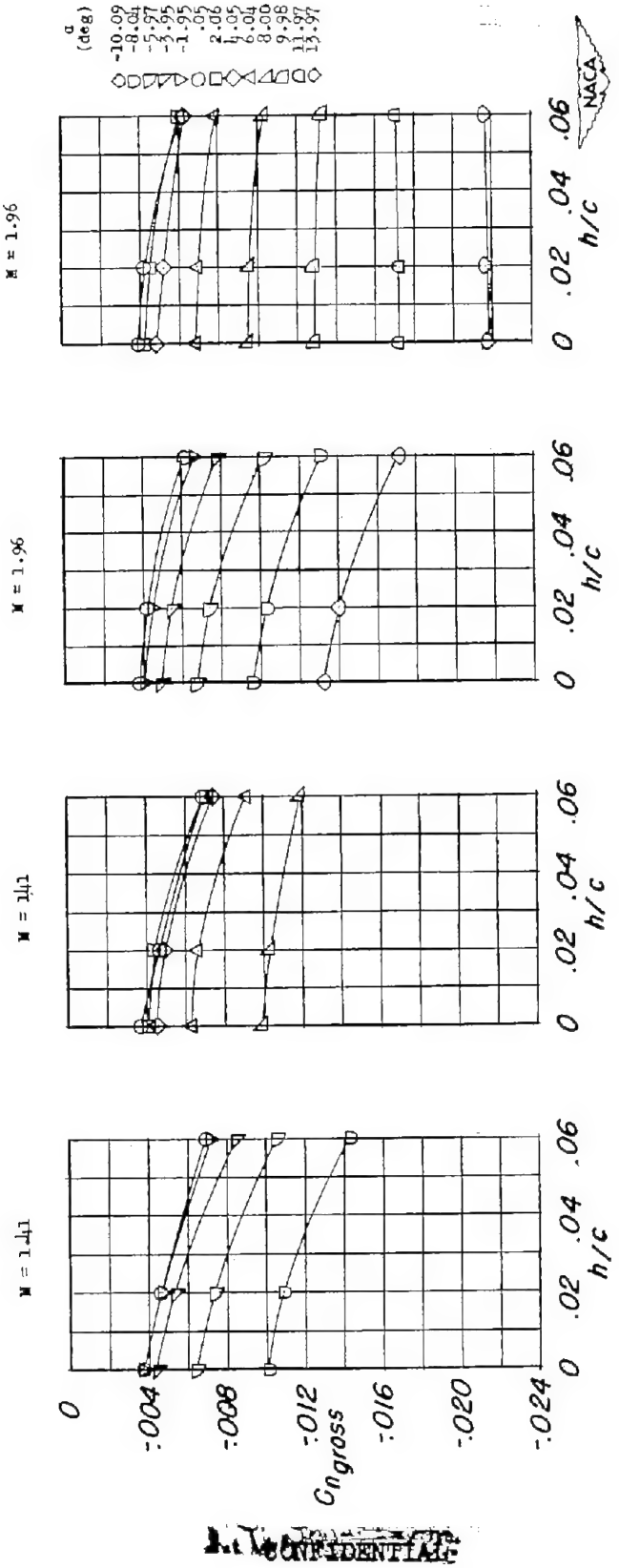

(c) $b_B = 0.25\frac{b}{2}$; $y_B = 0.20\frac{b}{2}$.

Figure 7.- Concluded.

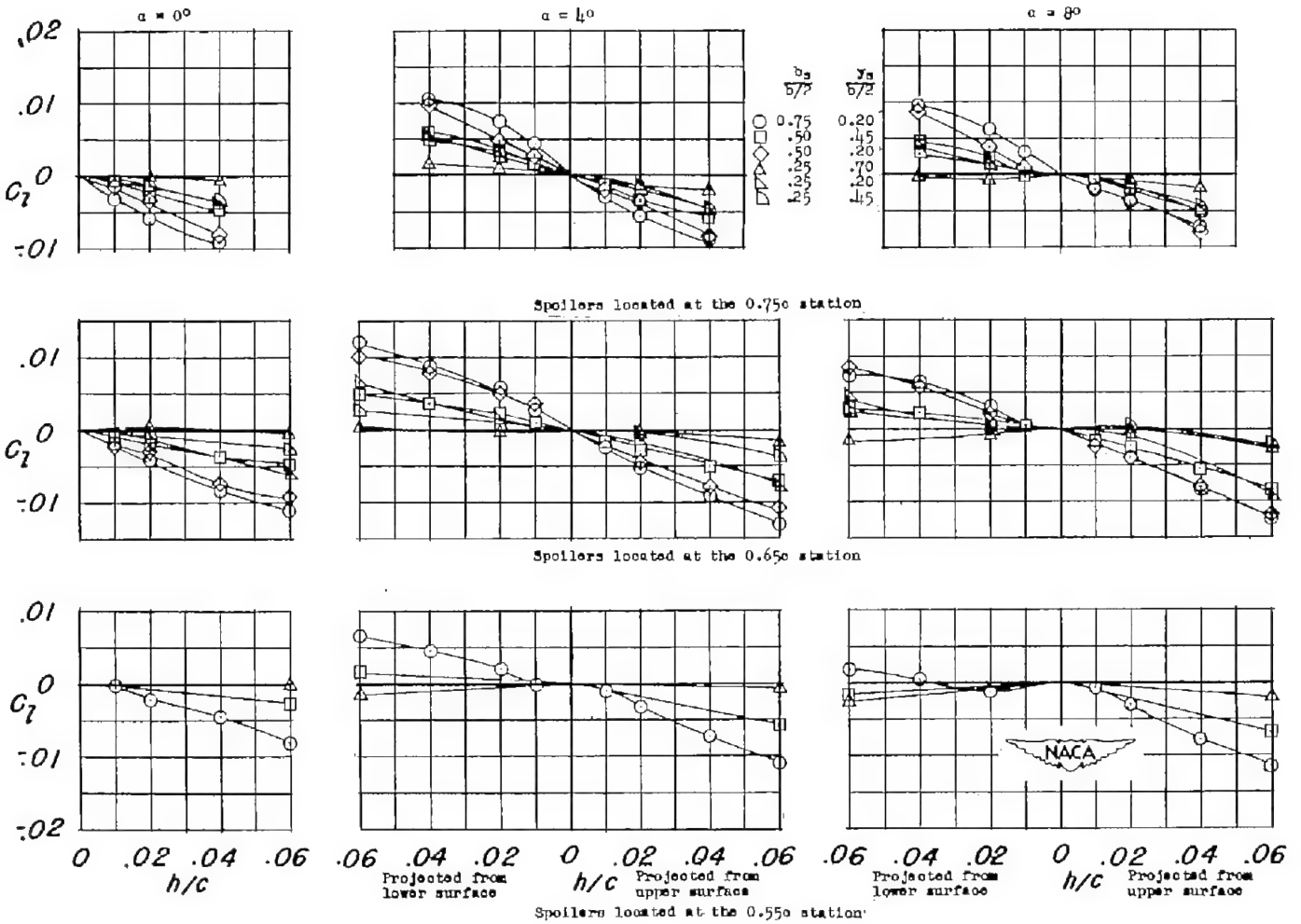

(a) M = 1.41; R = 2.1×10^6.

Figure 8.- Variation of rolling-moment coefficient with spoiler projection for all wing-spoiler combinations investigated.

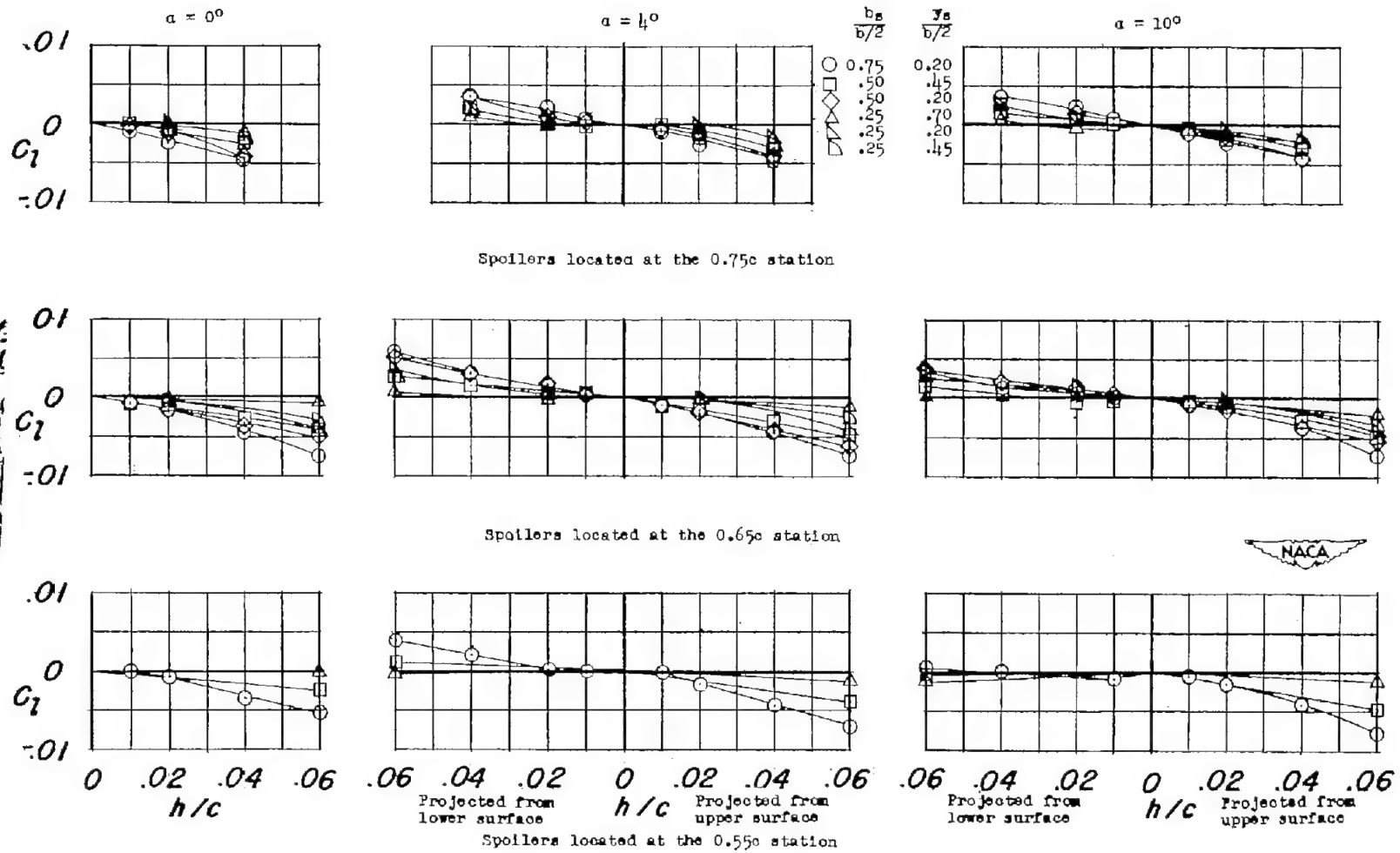

(b) M = 1.96; R = 1.7×10^6.

Figure 8.- Concluded.

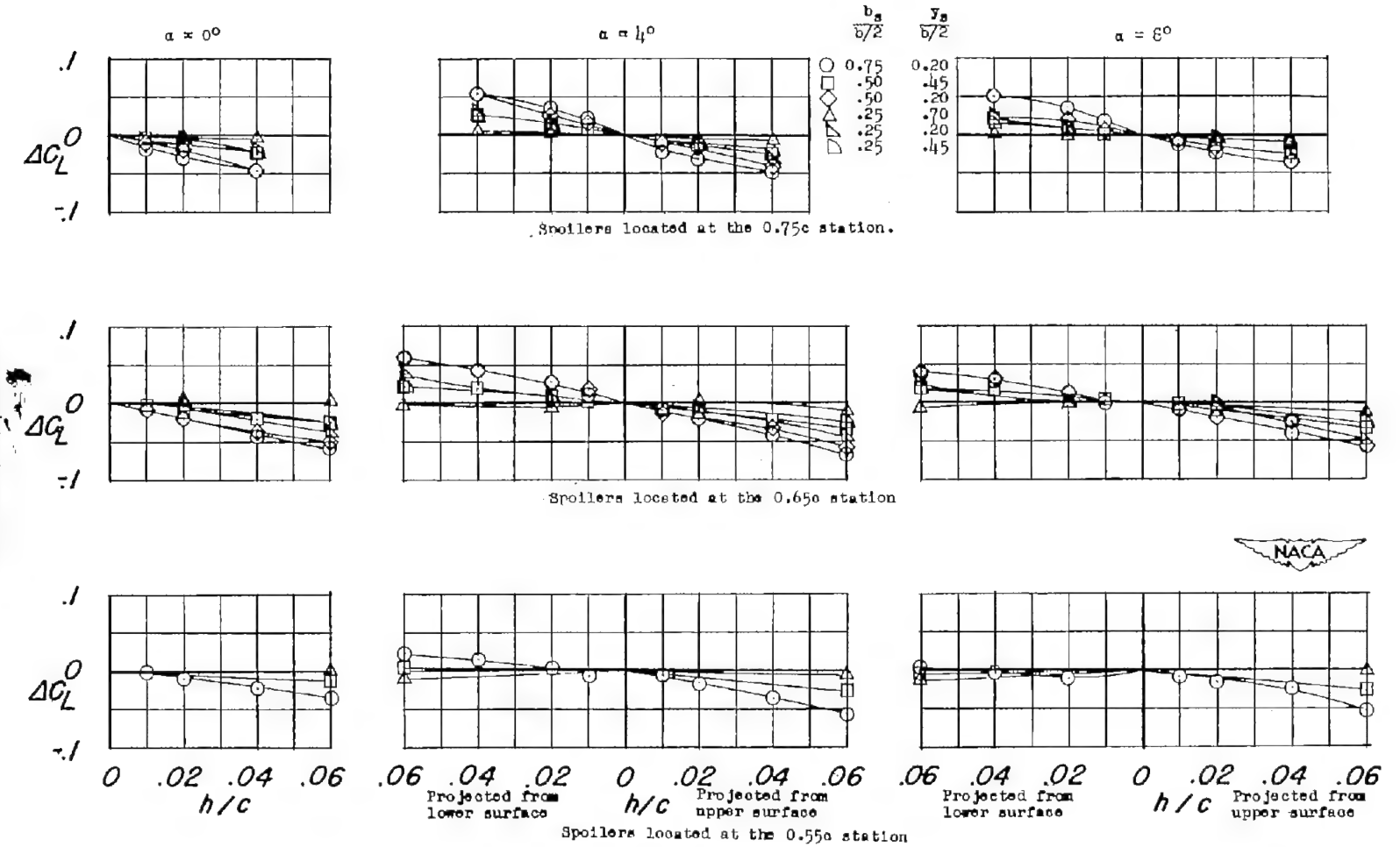

(a) M = 1.41; R = 2.1×10^6.

Figure 9.- Variation of incremental lift coefficient with spoiler projection for all wing-spoiler combinations investigated.

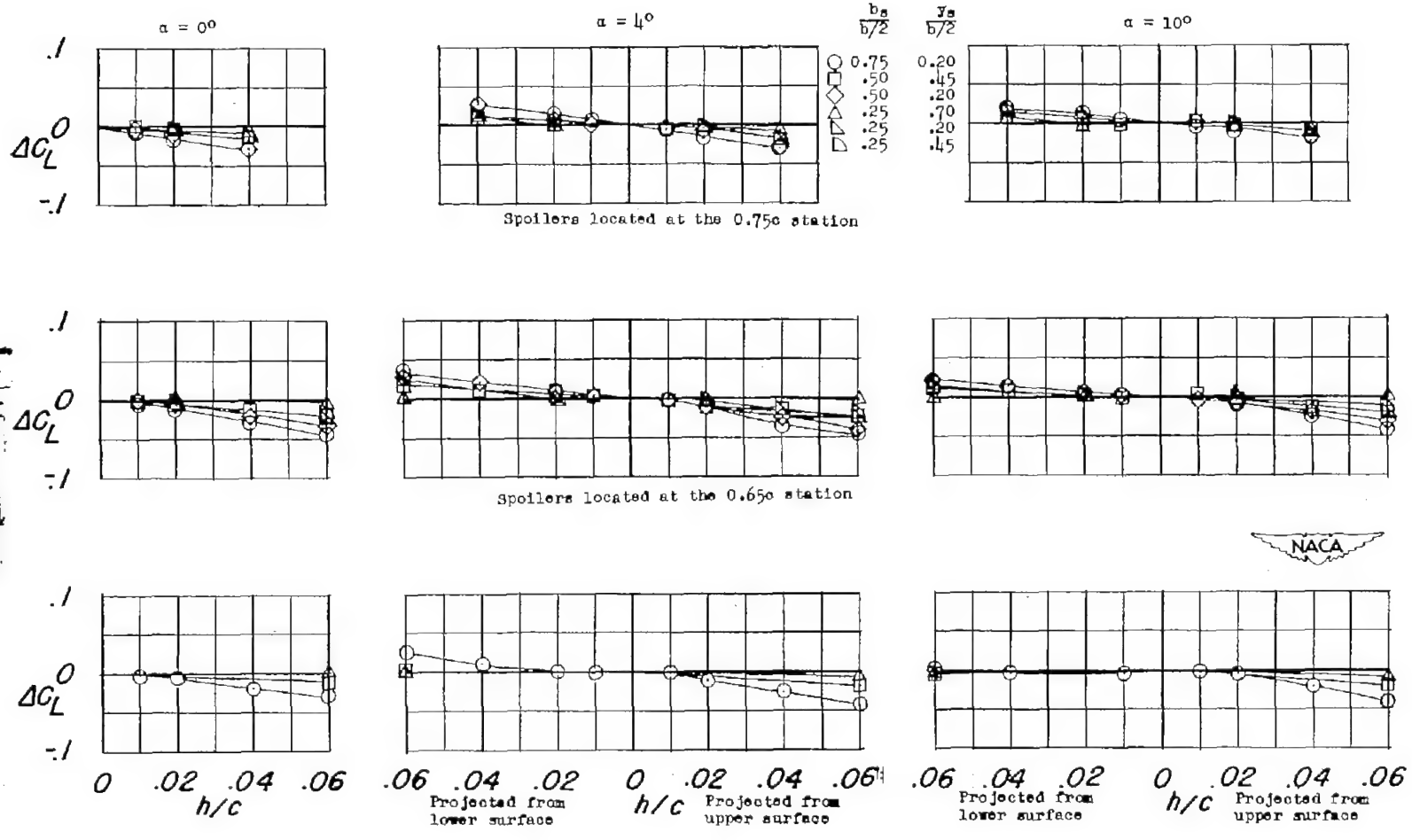

(b) M = 1.96; R = 1.7×10^6.

Figure 9.- Concluded.

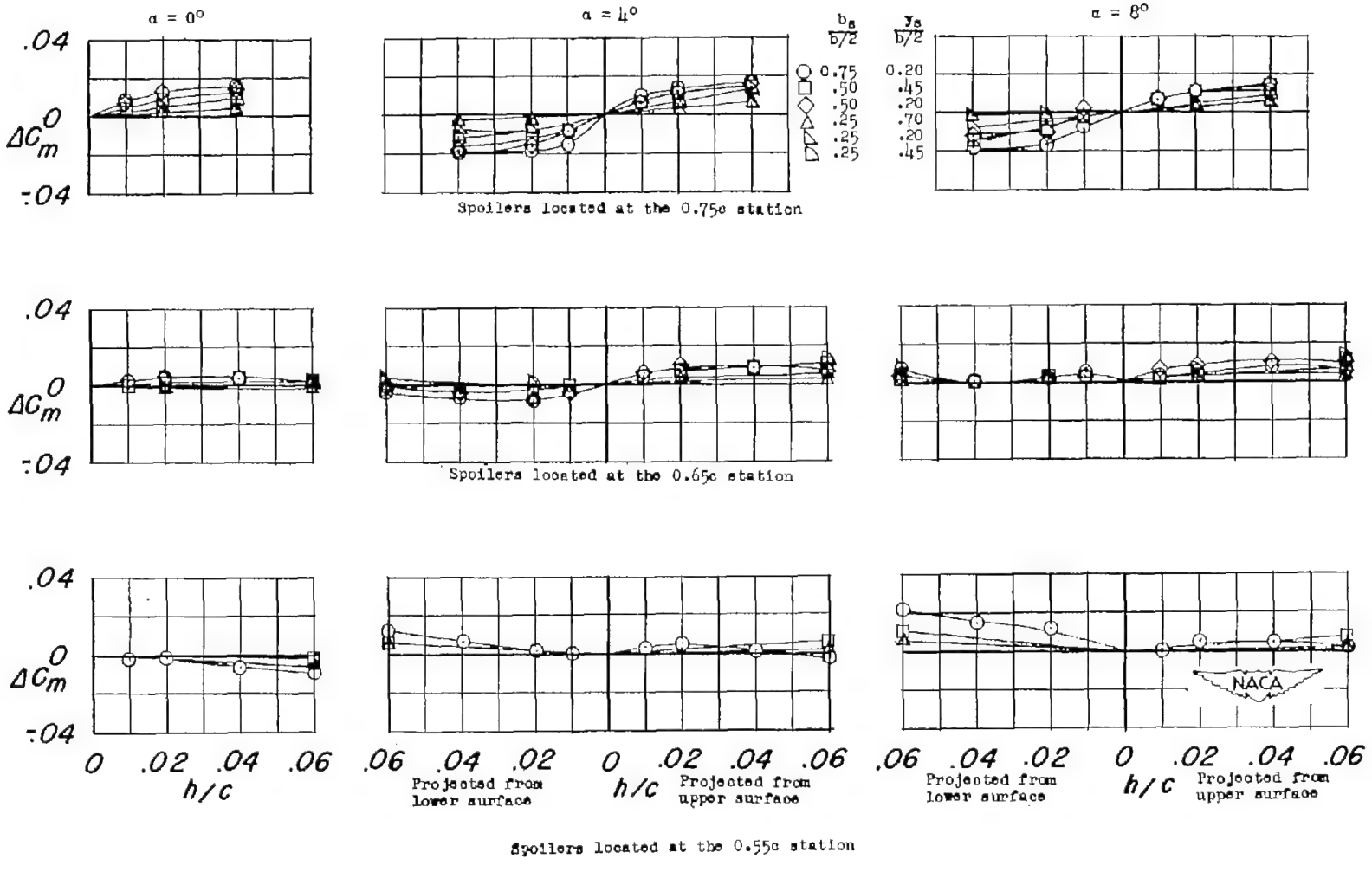

(a) M = 1.41; R = 2.1×10^6.

Figure 10.- Variation of incremental pitching-moment coefficient with spoiler projection for all wing-spoiler combinations investigated.

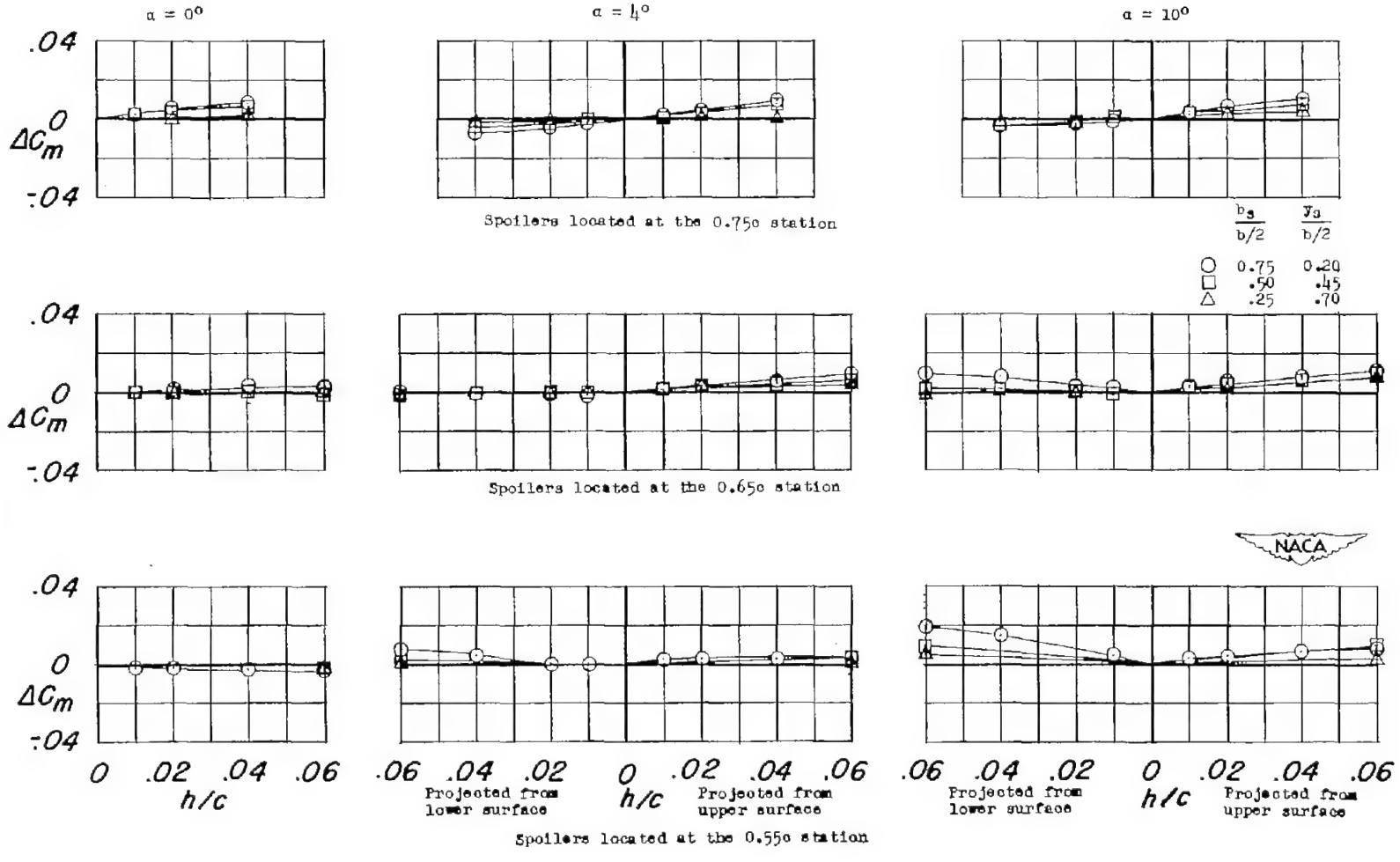

(b) M = 1.96; R = 1.7×10^6.

Figure 10.- Continued.

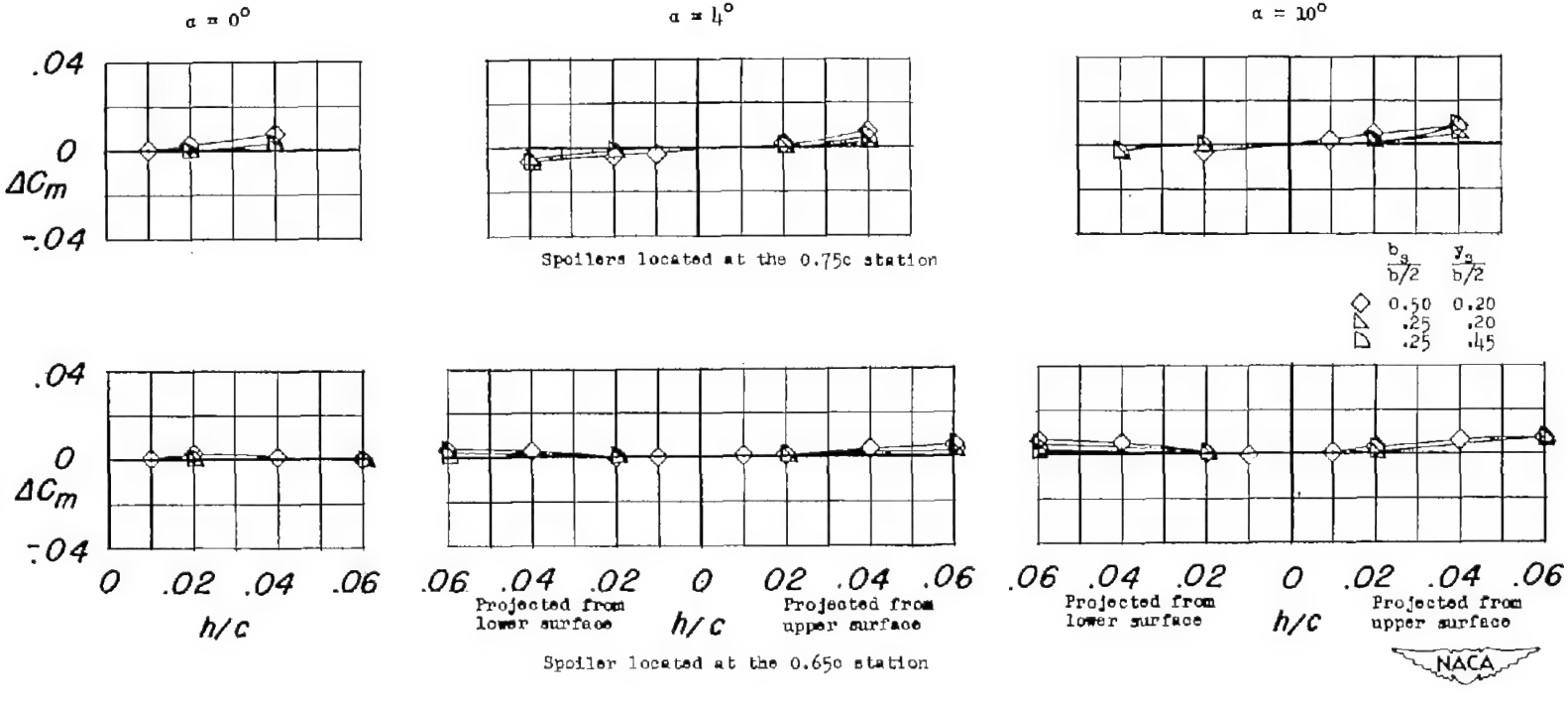

(b) Concluded.

Figure 10.- Concluded.

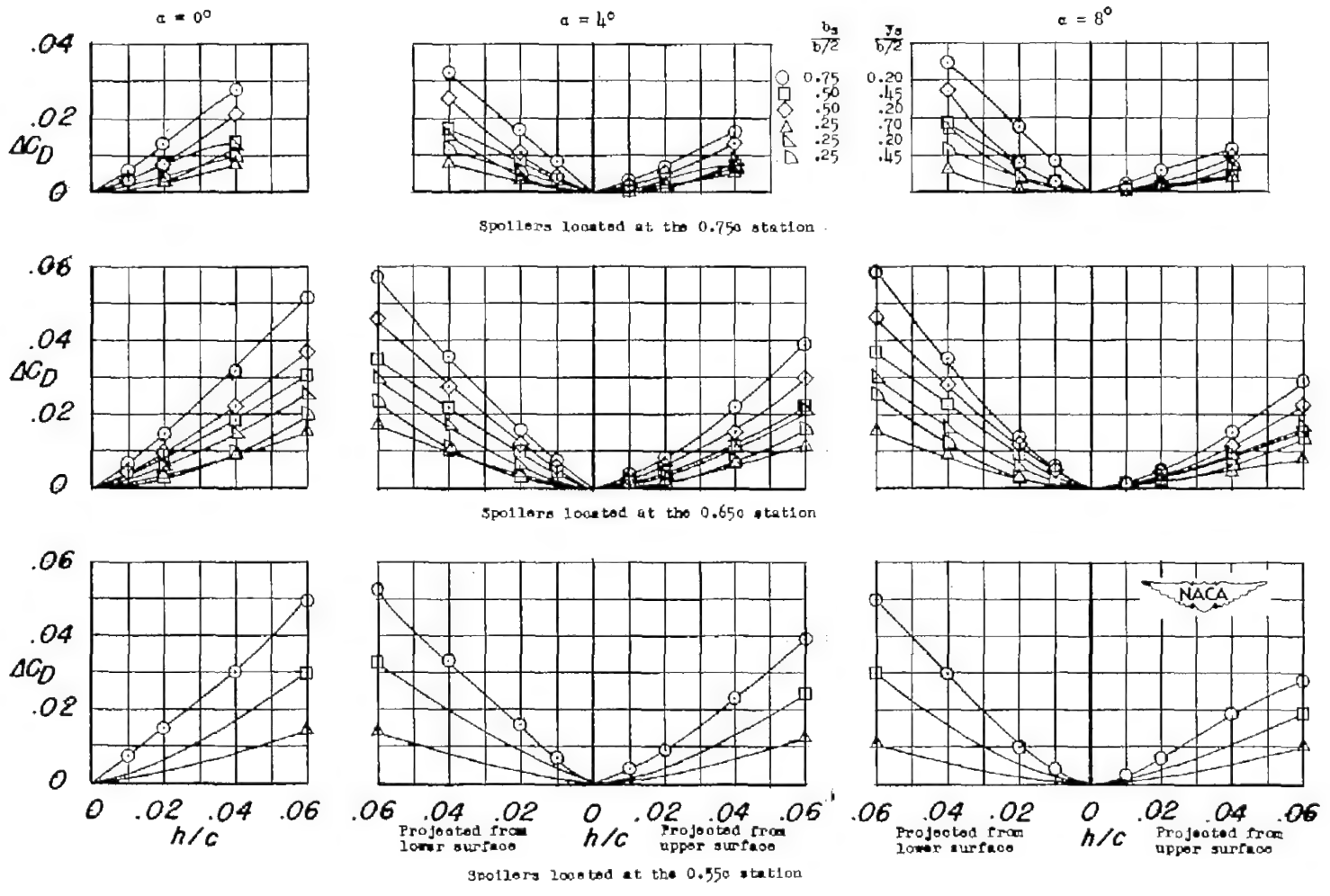

(a) M = 1.41; R = 2.1×10^6.

Figure 11.- Variation of incremental drag coefficient with spoiler projection for all wing-spoiler combinations investigated.

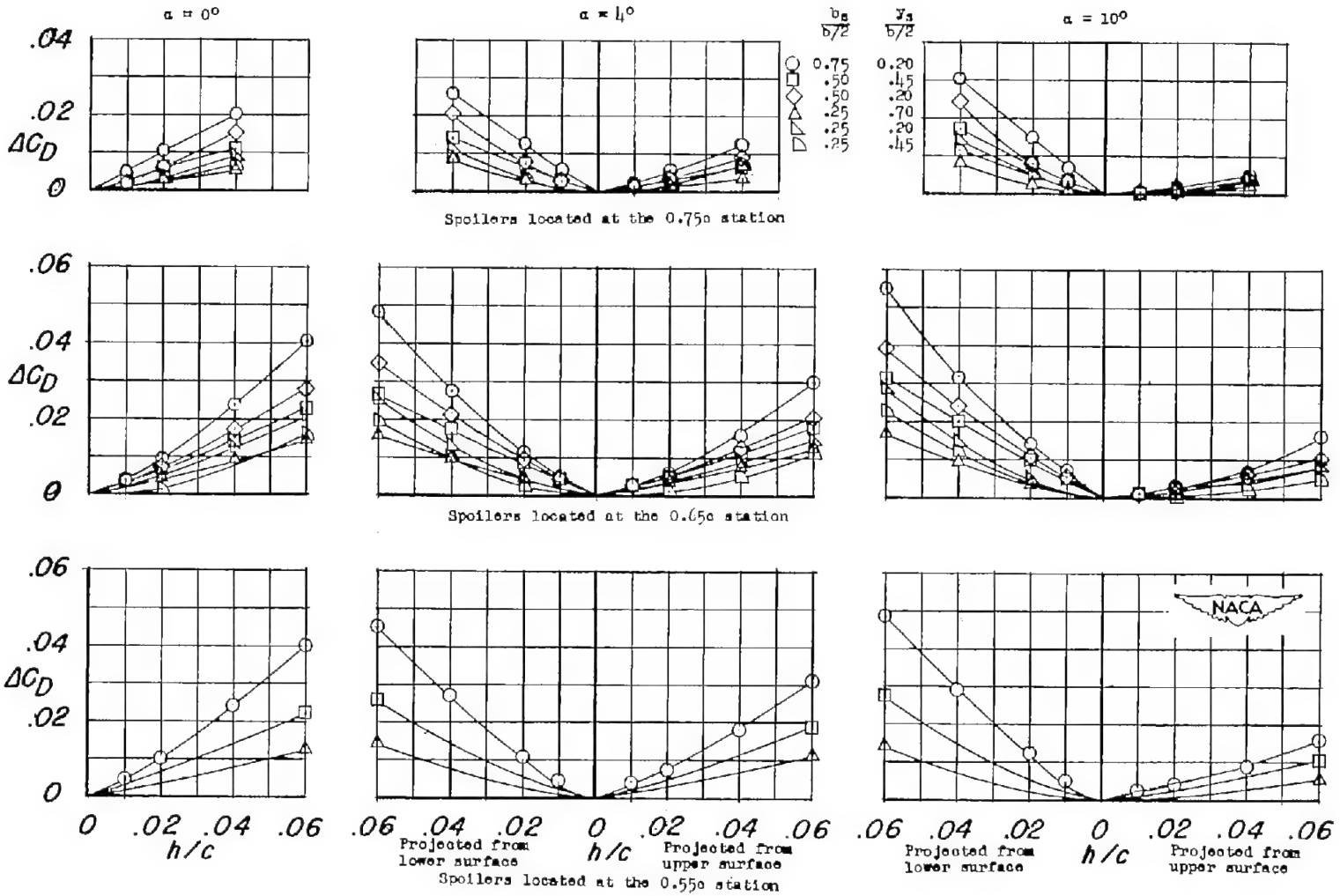

(b) M = 1.96; R = 1.7×10^6.

Figure 11.- Concluded.

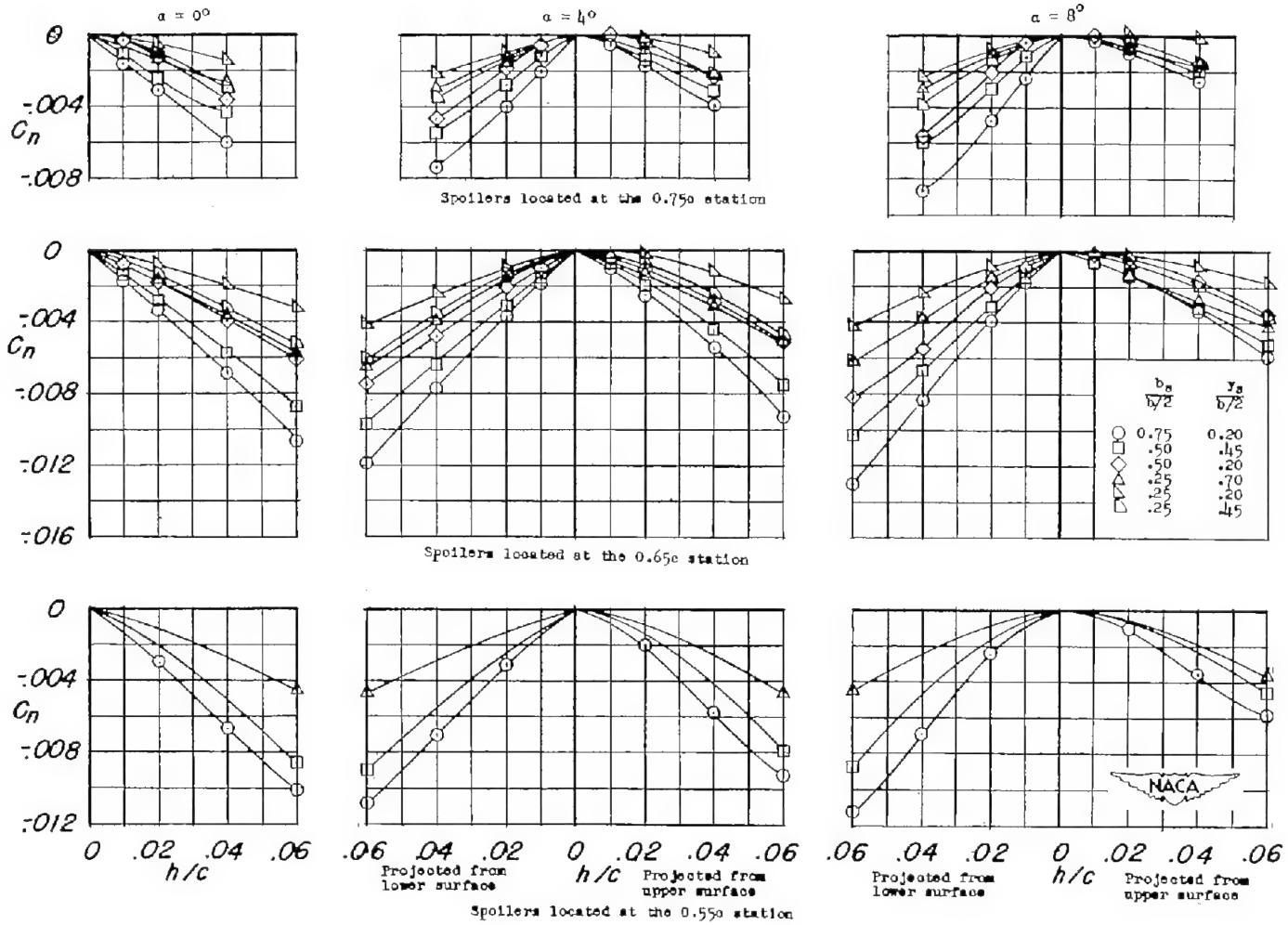

(a) M = 1.41; R = 2.1×10^6.

Figure 12.- Variation of yawing-moment coefficient with spoiler projection for all wing-spoiler combinations investigated.

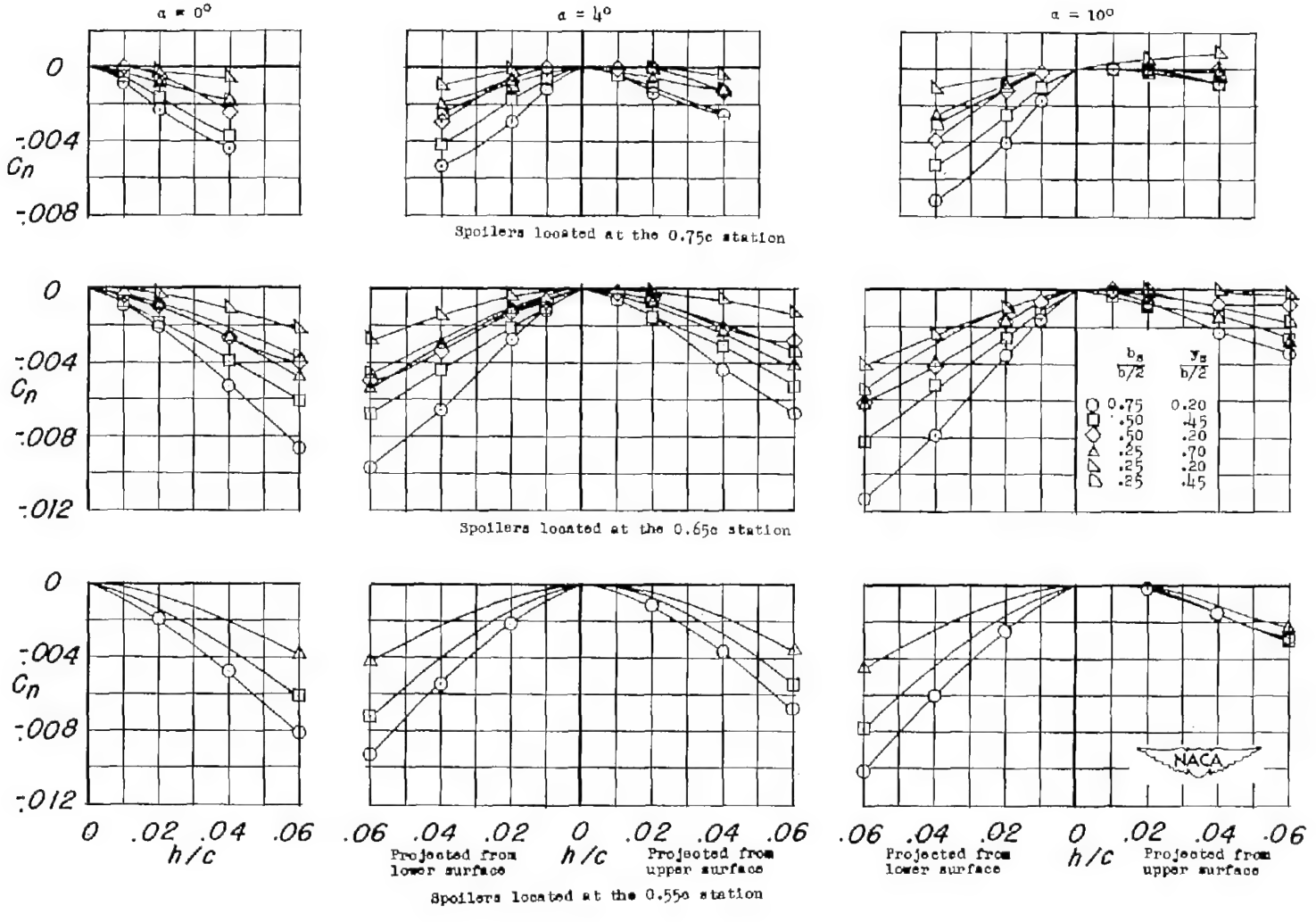

(b) M = 1.96; R = 1.7×10^6.

Figure 12.- Concluded.

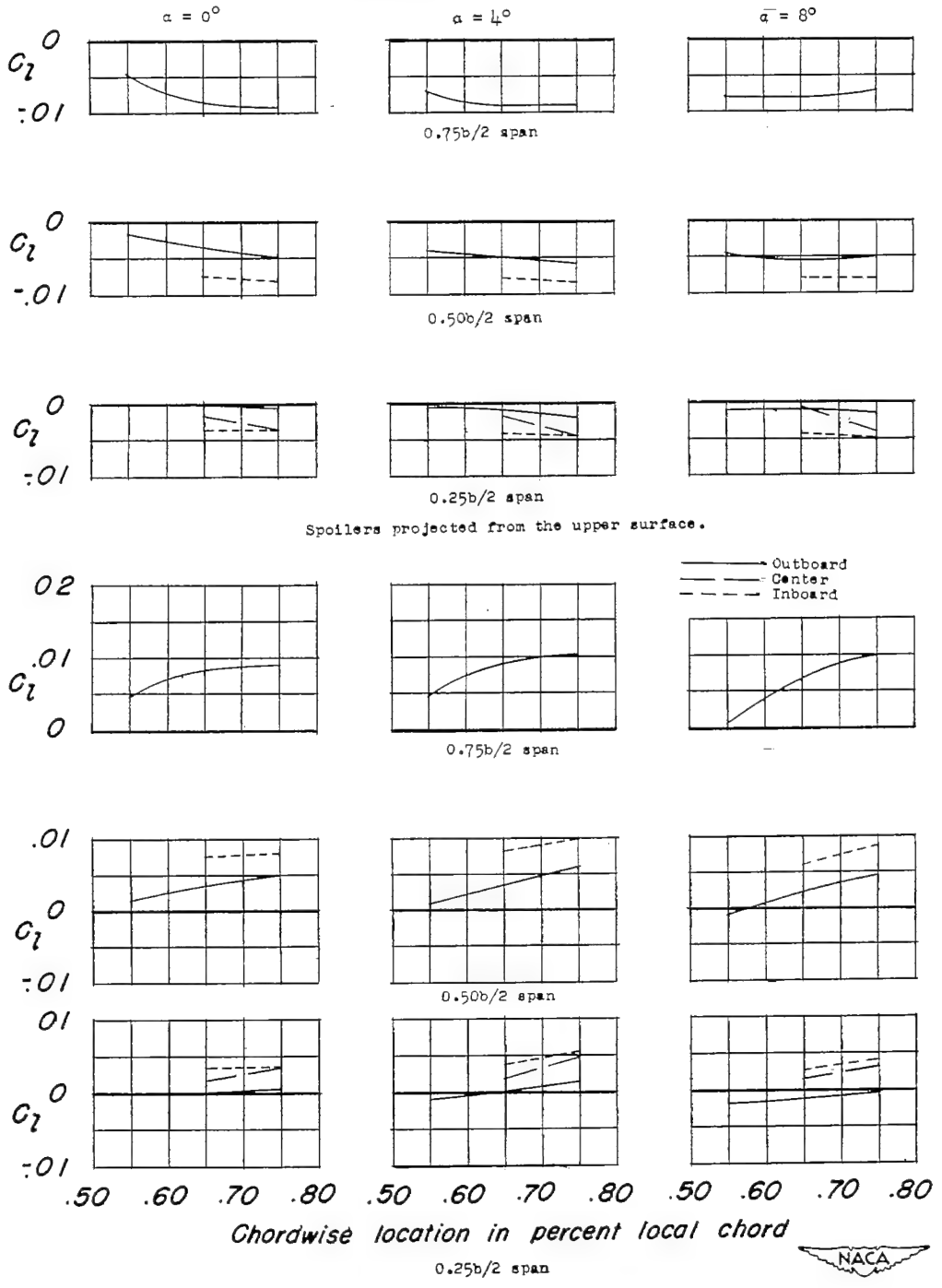

(a) M = 1.41.

Figure 13.- Variation of rolling-moment coefficient with spoiler chordwise location for h/c = 0.04.

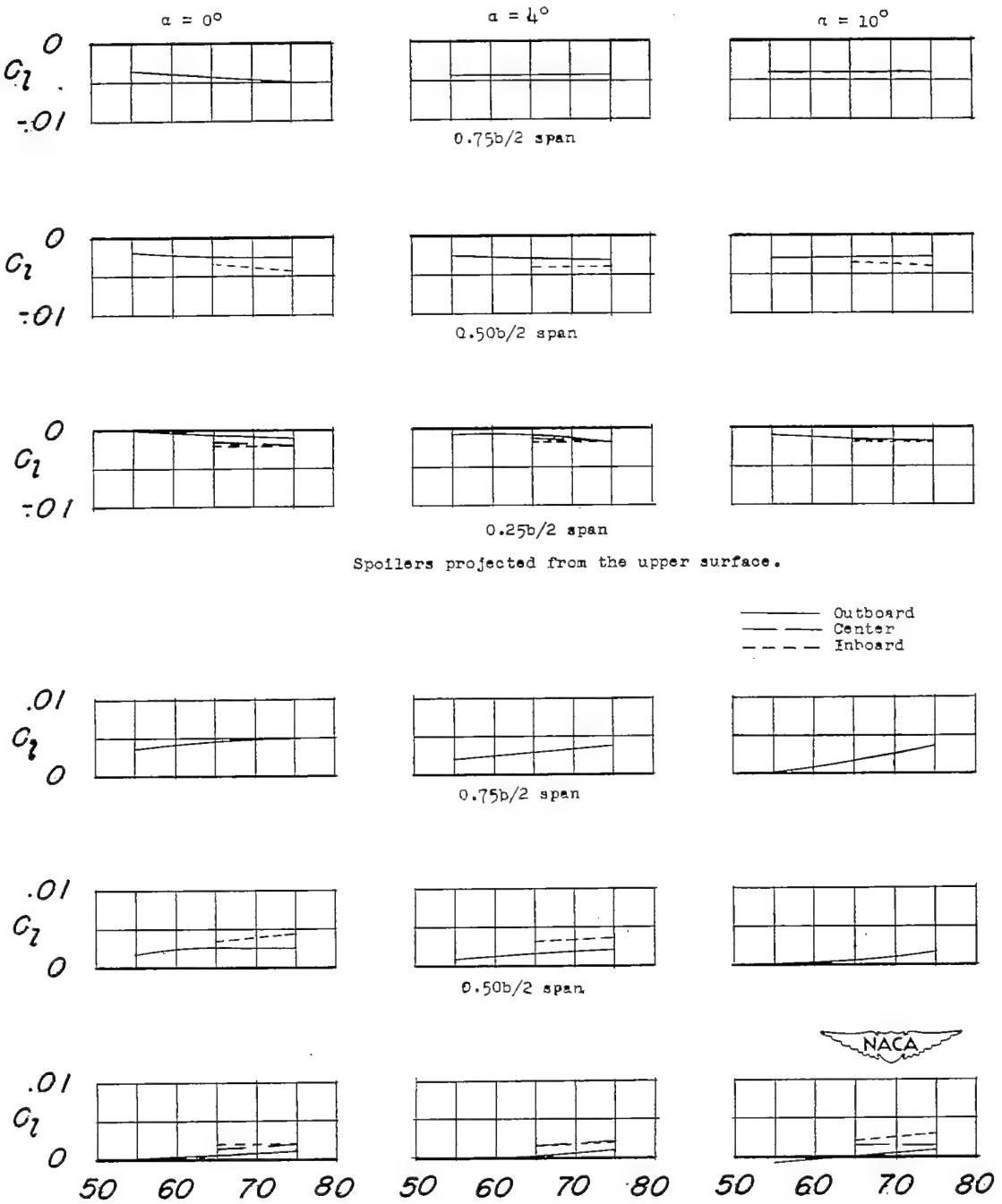

Spoilers projected from the upper surface.

Spoilers projected from the lower surface.

(b) M = 1.96.

Figure 13.- Concluded.

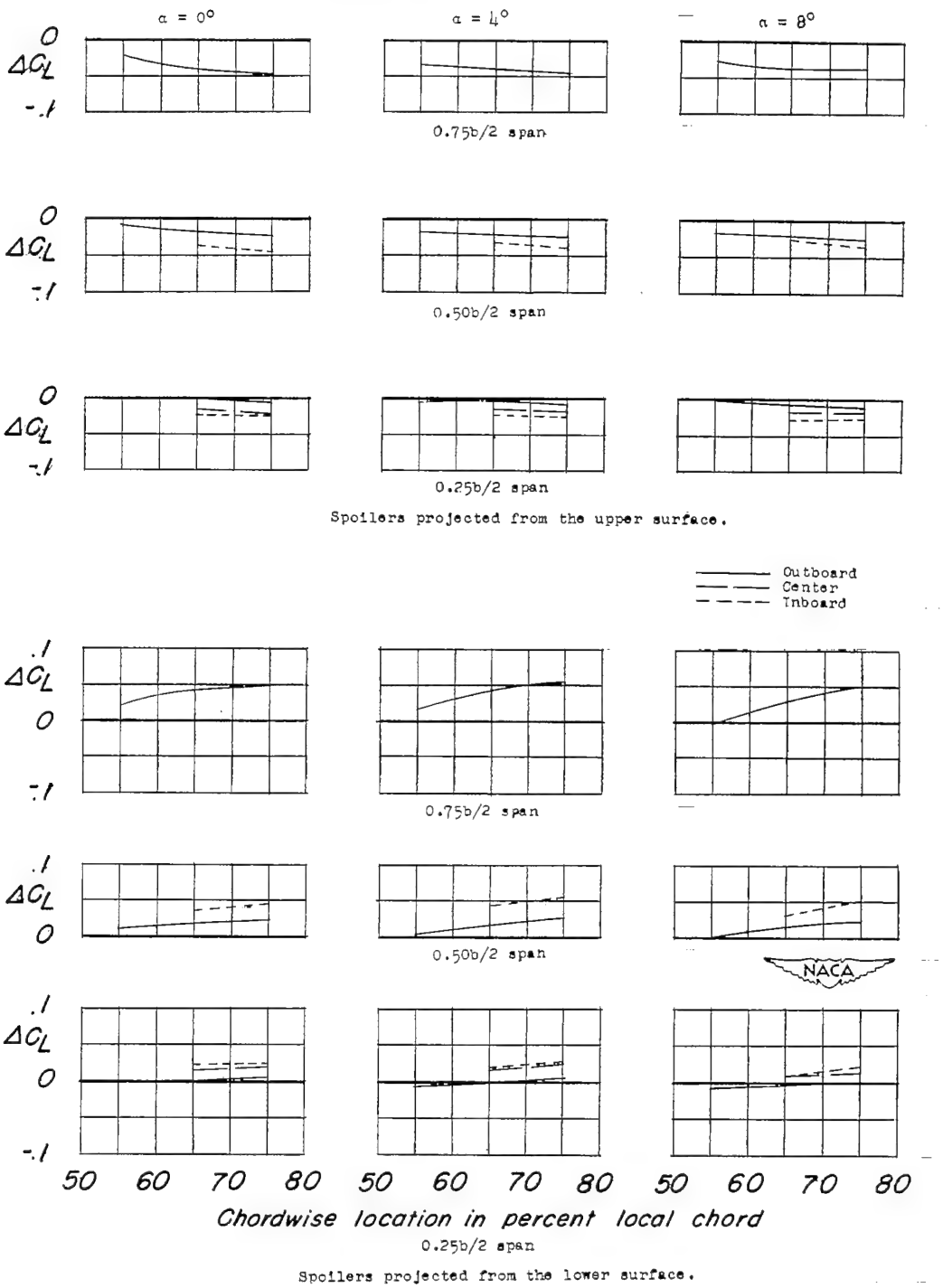

(a) M = 1.41.

Figure 14.- Variation of incremental lift coefficient with spoiler chordwise location for h/c = 0.04.

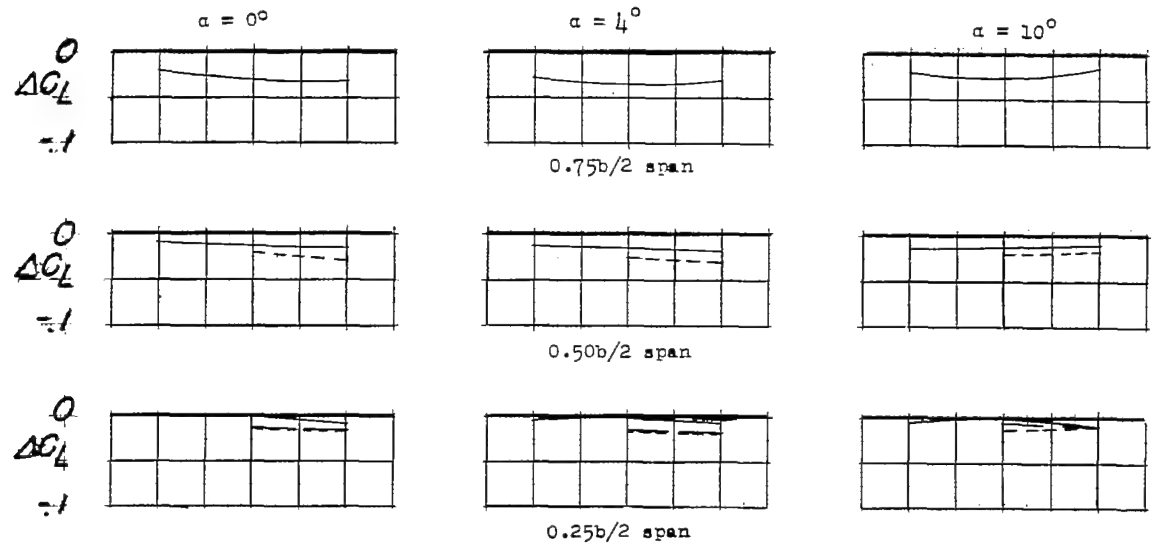

Spoilers projected from the upper surface.

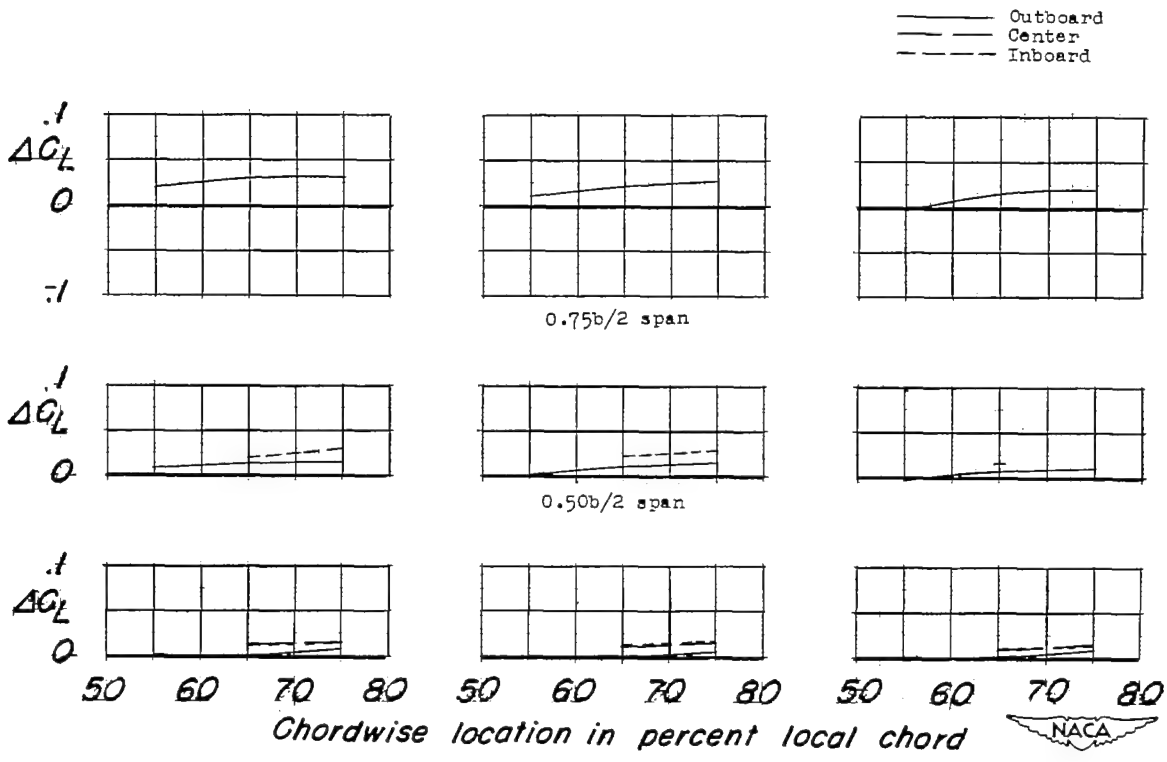

Spoilers projected from the lower surface.

(b) M = 1.96.

Figure 14.- Concluded.

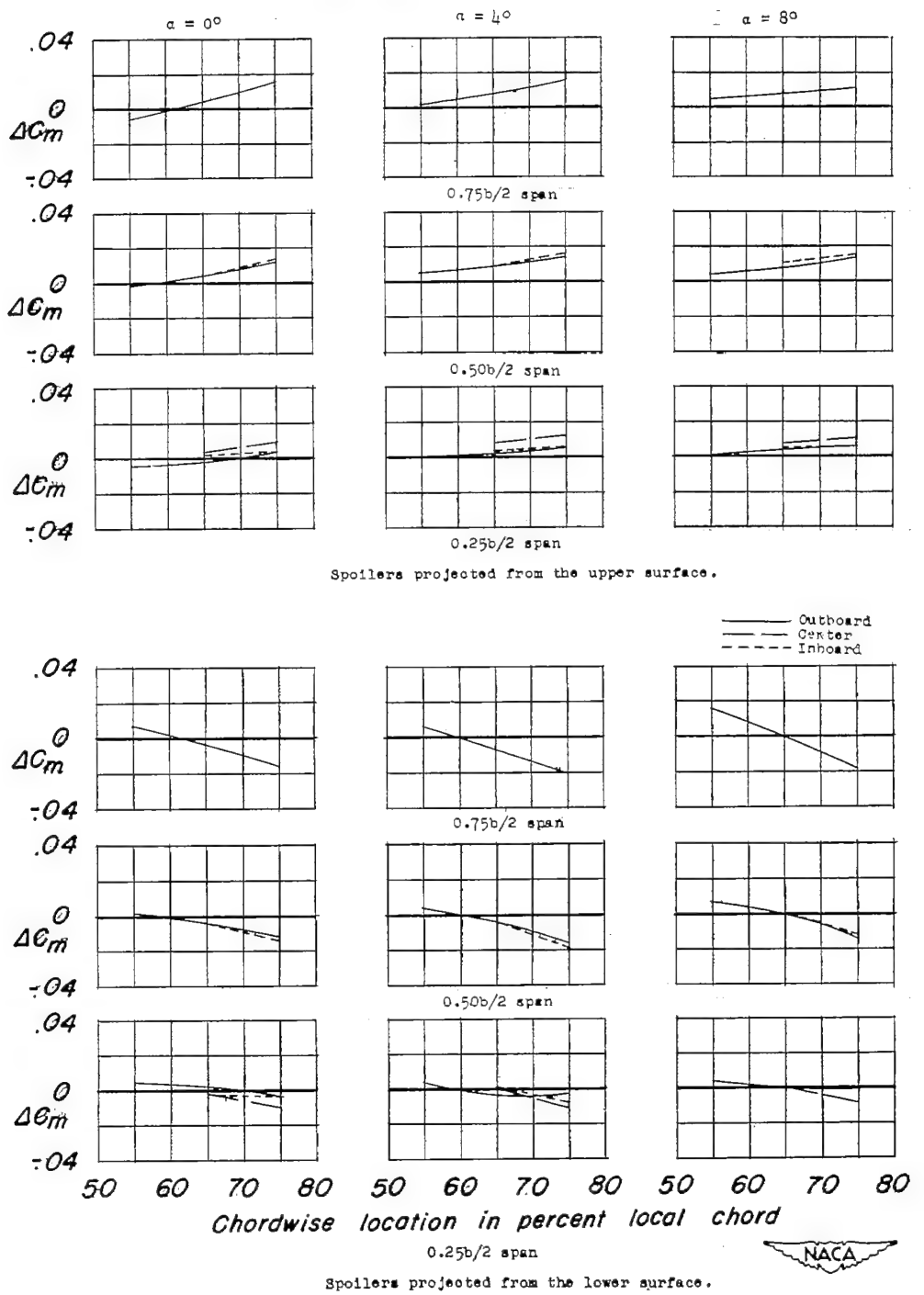

(a) M = 1.41.

Figure 15.- Variation of incremental pitching-moment coefficient with spoiler chordwise location for h/c = 0.04.

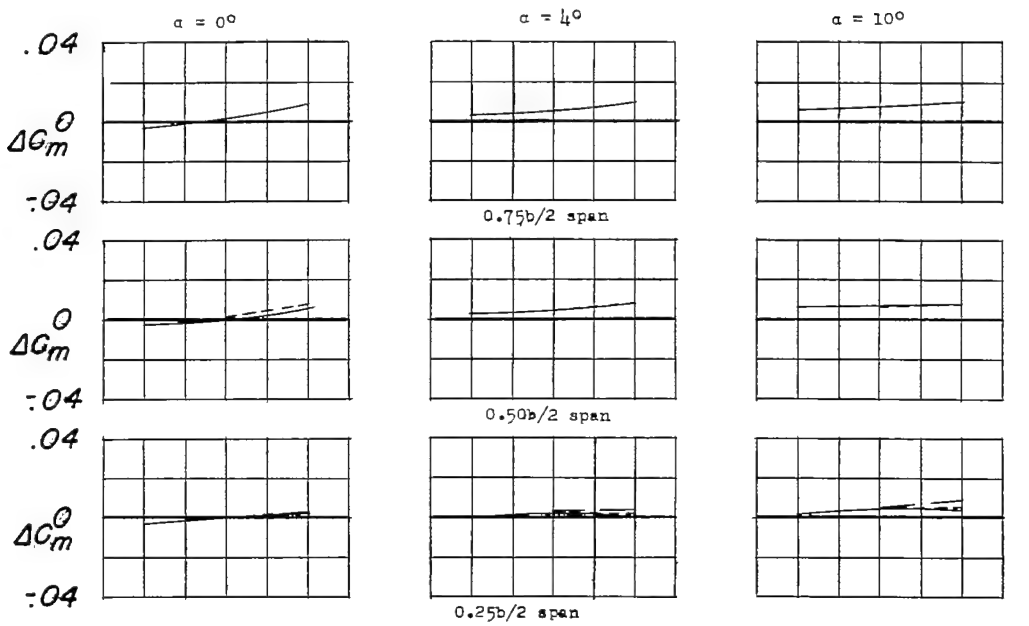

Spoilers projected from the upper surface.

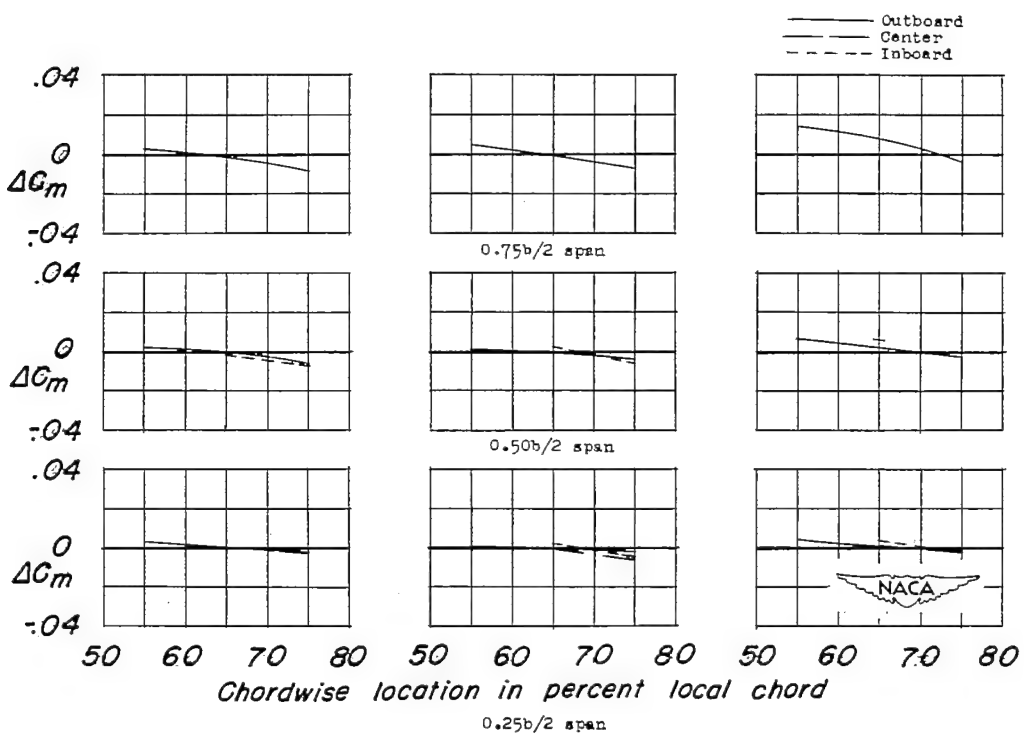

Spoilers projected from the lower surface.

(b) M = 1.96.

Figure 15.- Concluded.

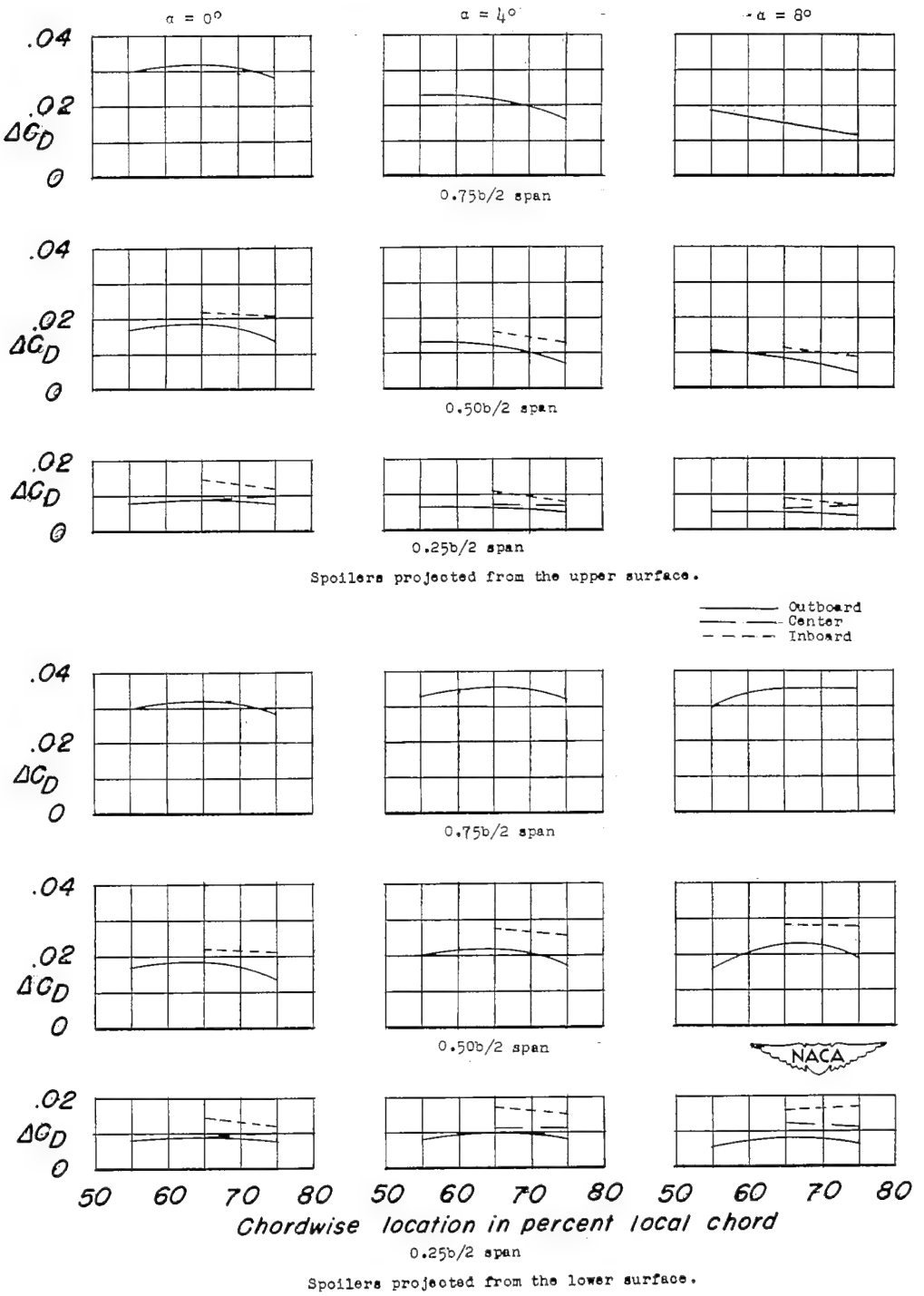

(a) M = 1.41.

Figure 16.- Variation of incremental drag coefficient with spoiler chordwise location for h/c = 0.04.

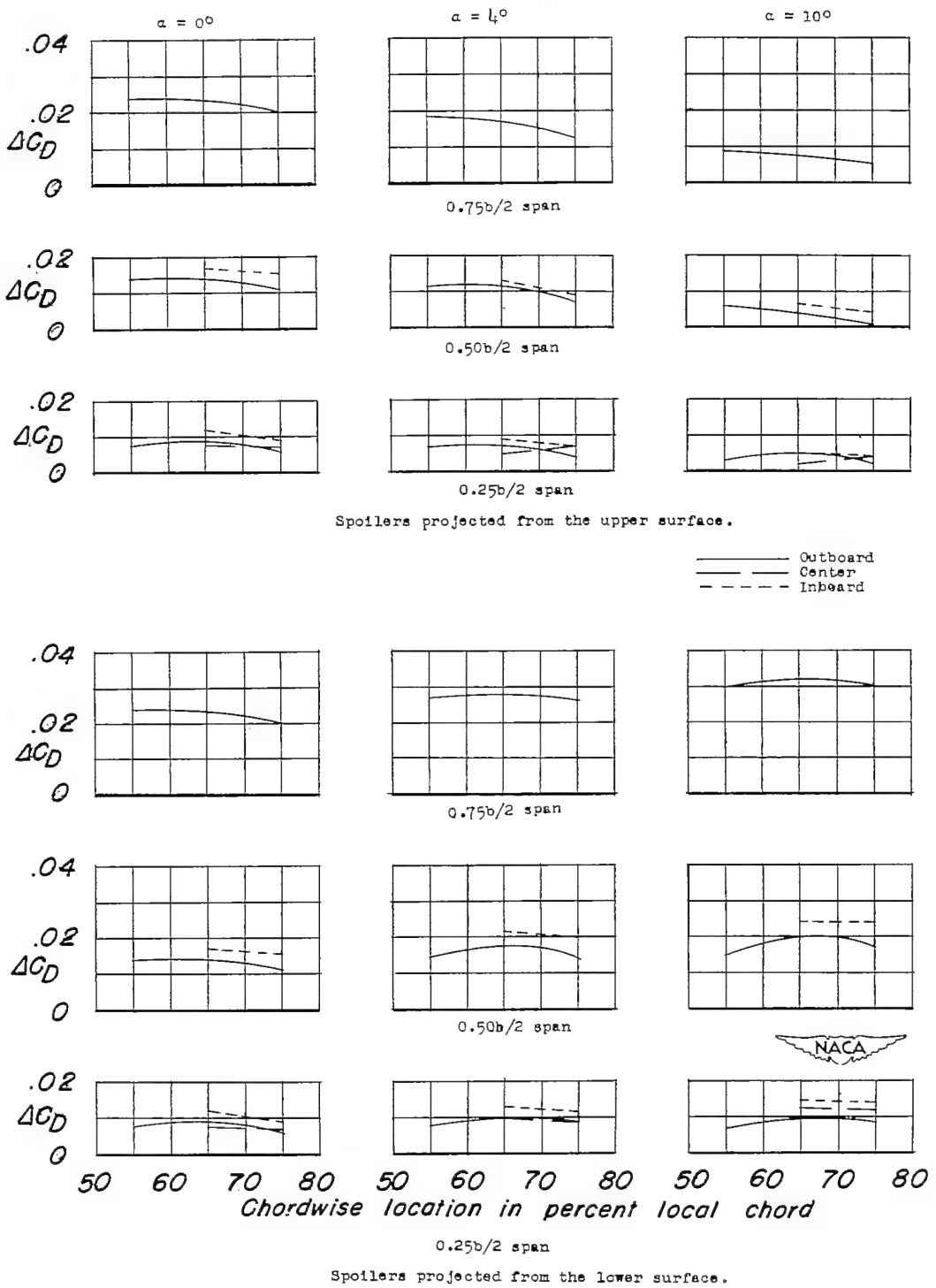

Spoilers projected from the upper surface.

Spoilers projected from the lower surface.

(b) M = 1.96.

Figure 16.- Concluded.

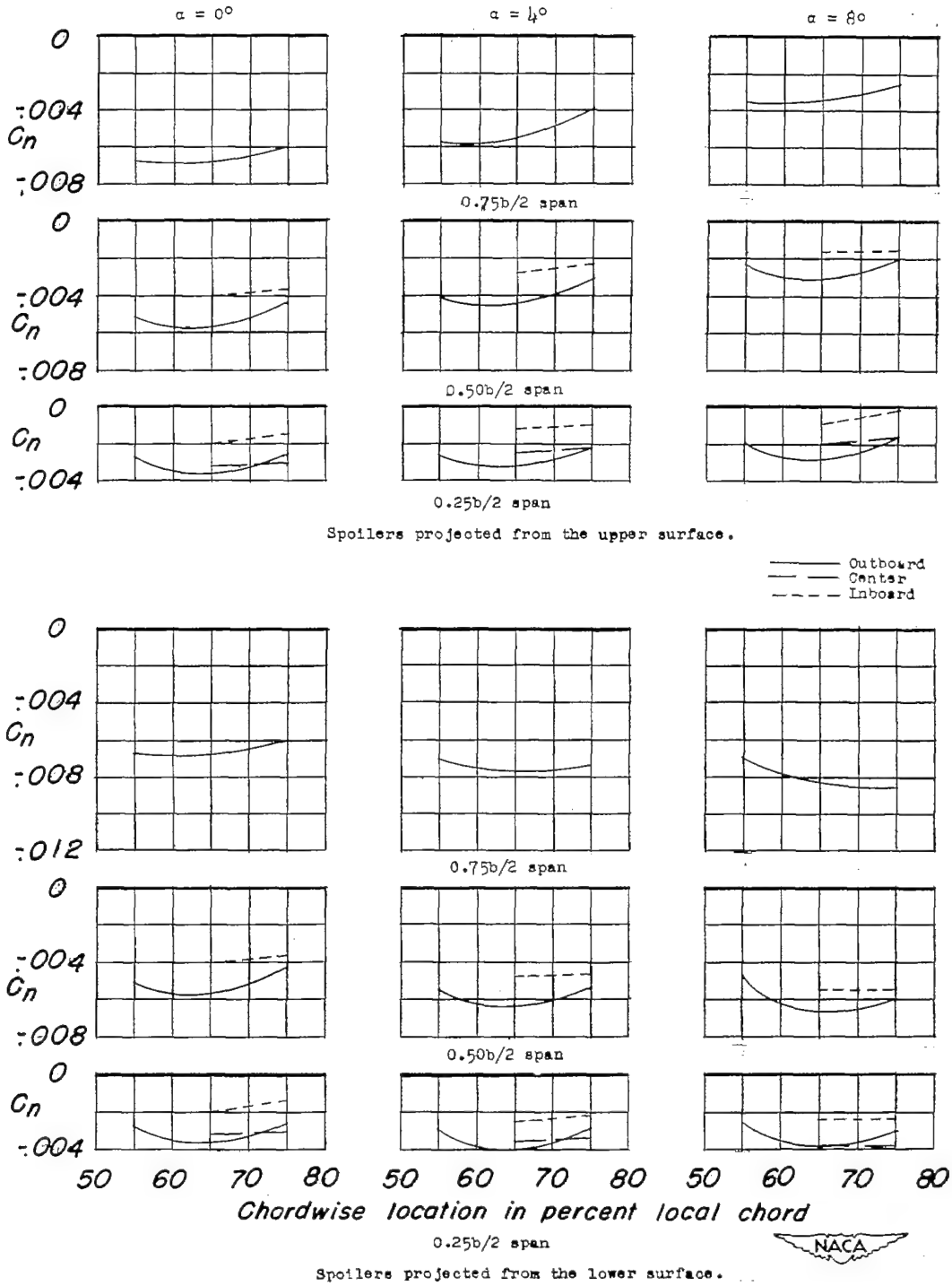

(a) M = 1.41.

Figure 17.- Variation of yawing-moment coefficient with spoiler chordwise location for h/c = 0.04.

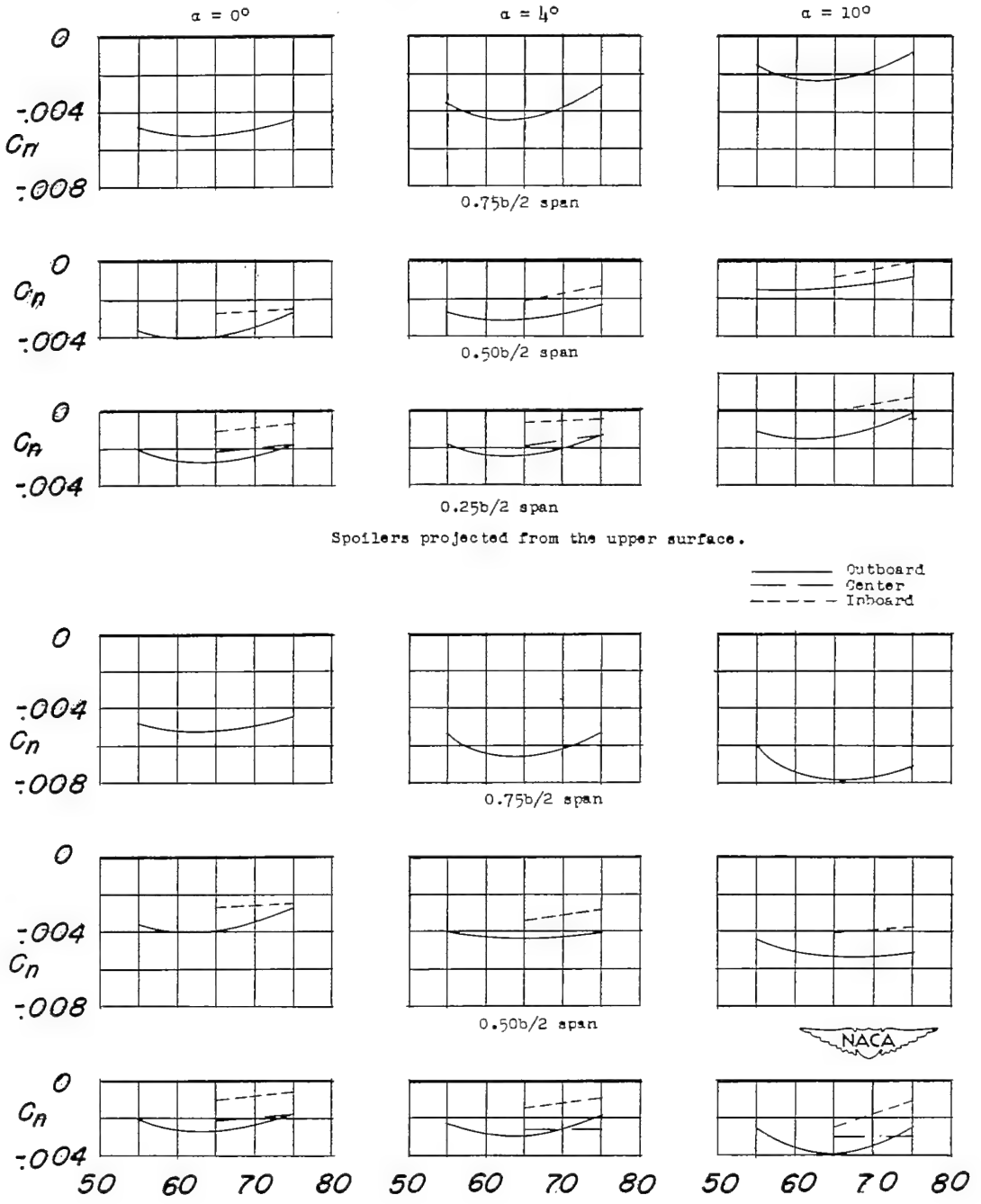

Spoilers projected from the upper surface.

Spoilers projected from the lower surface.

(b) M = 1.96.

Figure 17.- Concluded.

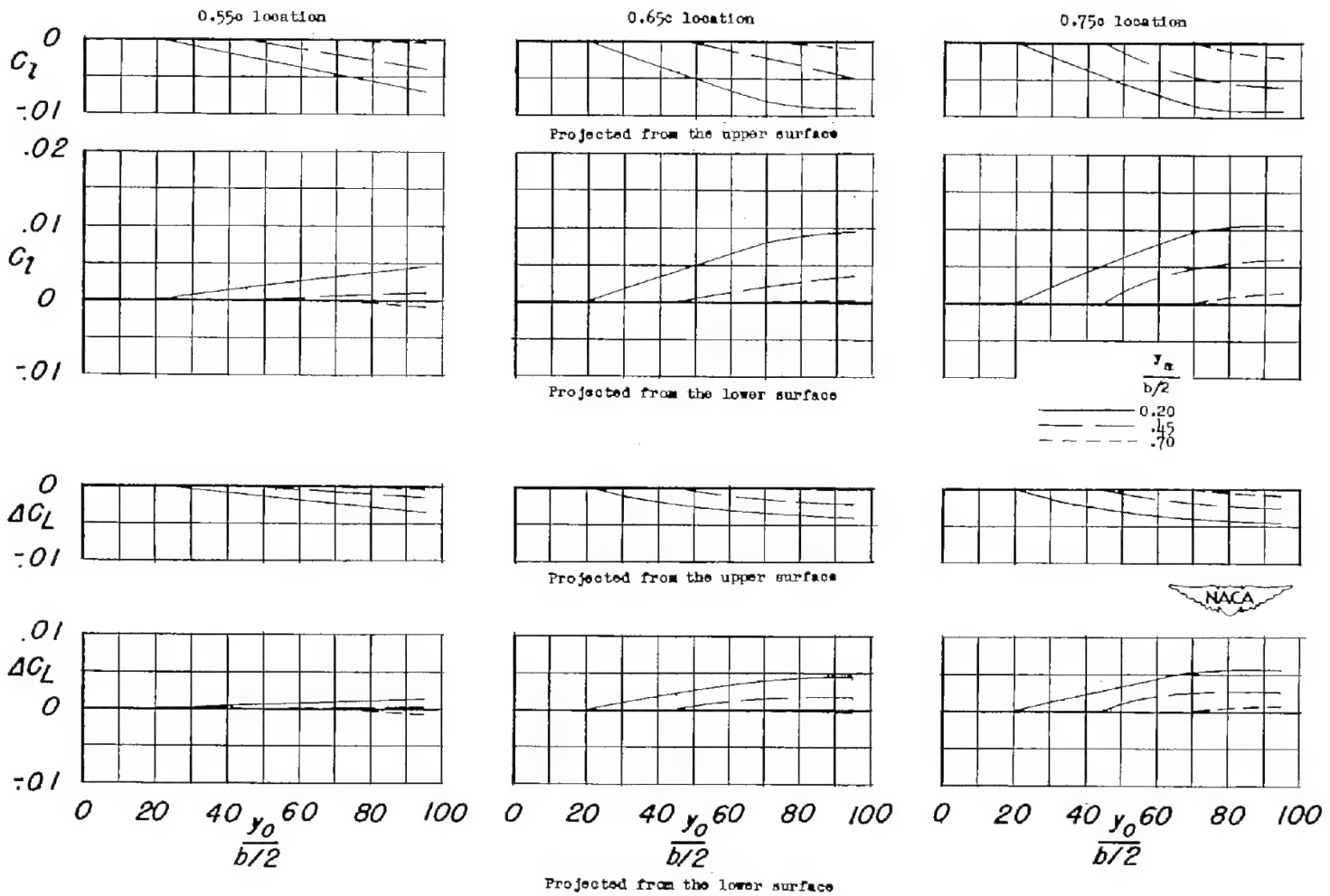

(a) M = 1.41.

Figure 18.- Variation of rolling-moment and incremental lift coefficient with spoiler span and spanwise location. h/c = 0.04, $\alpha = 4^\circ$.

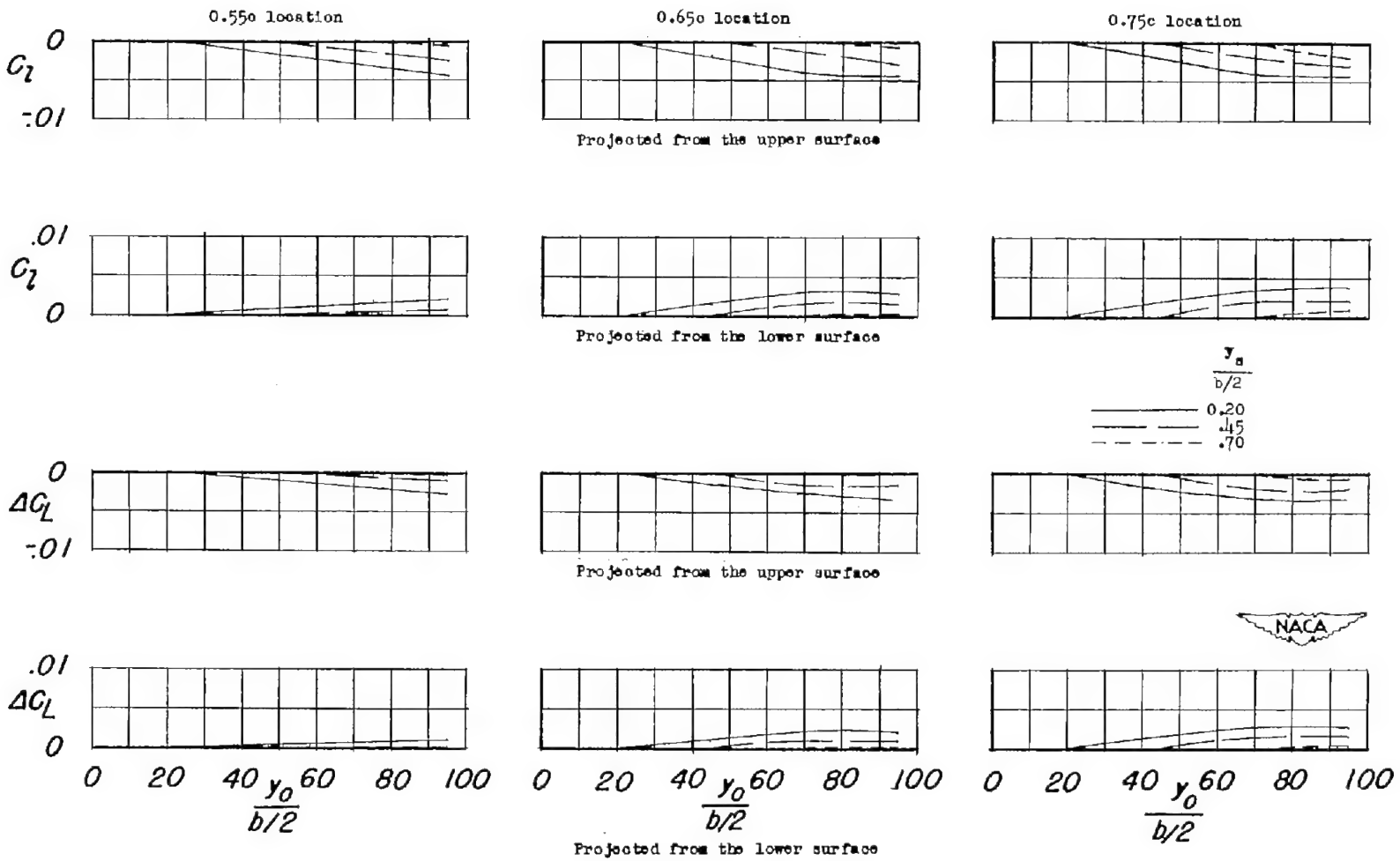

(b) M = 1.96.

Figure 18.- Concluded.

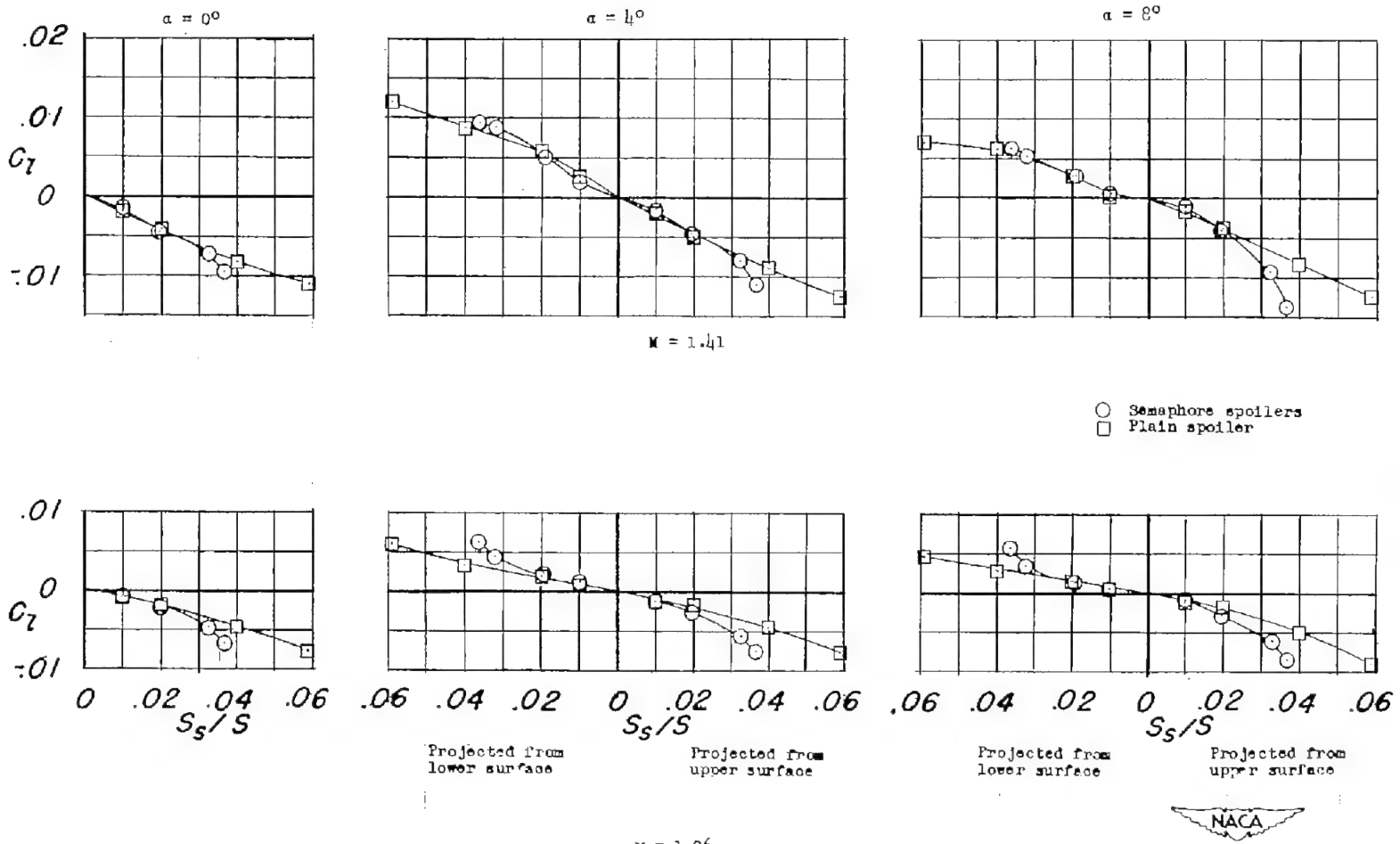

Figure 19.- Variation of rolling-moment coefficient with ratio of spoiler area to semispan wing area S_s/S for a $0.75\frac{b}{2}$- span plain spoiler and a $0.75\frac{b}{2}$- span row of semaphore spoilers located at the 0.65c station.

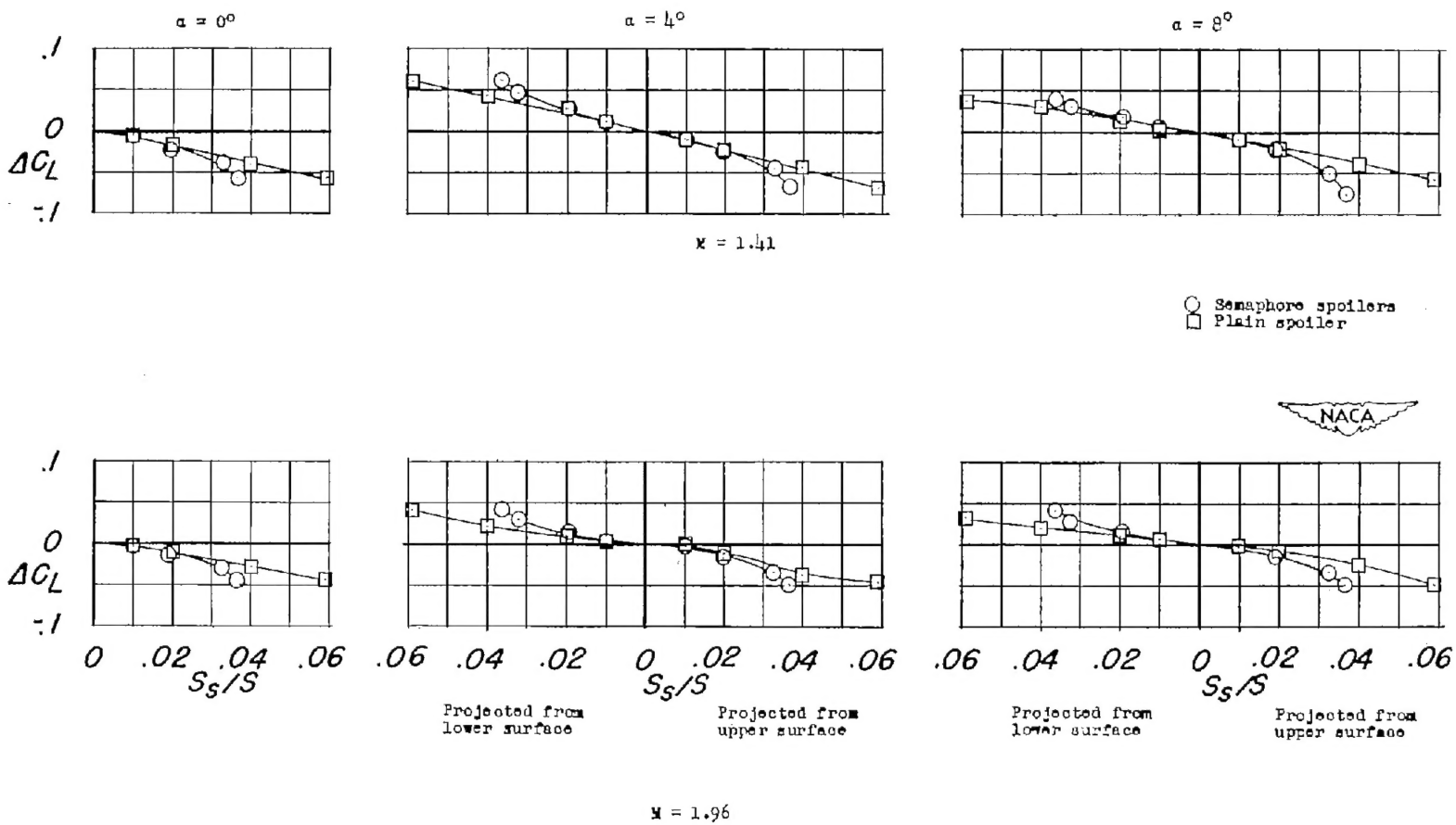

Figure 20.- Variation of incremental lift coefficient with ratio of spoiler area to semispan wing area S_s/S for a $0.75\frac{b}{2}$- span plain spoiler and a $0.75\frac{b}{2}$- span row of semaphore spoilers located at the 0.65c station.

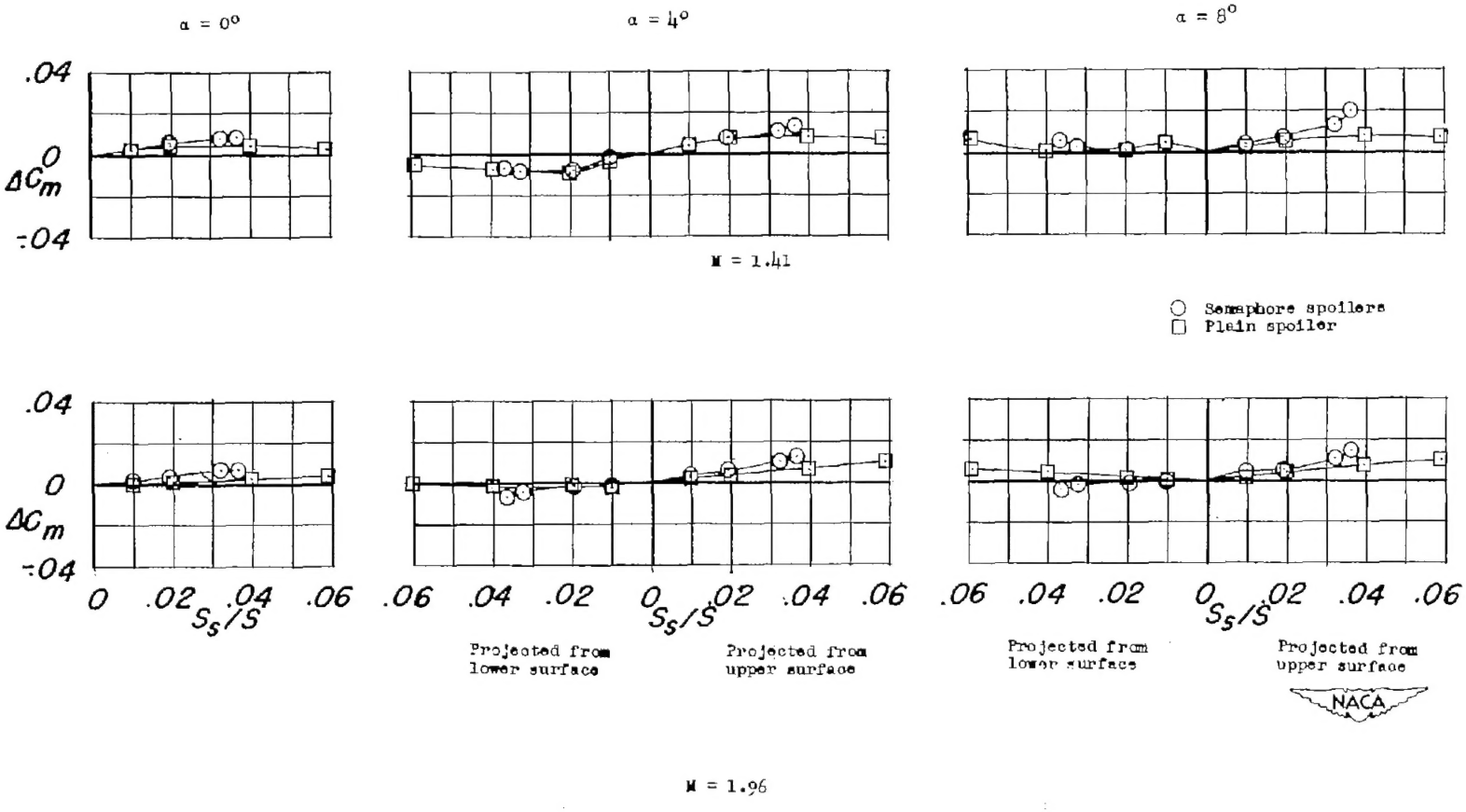

Figure 21.- Variation of incremental pitching-moment coefficient with ratio of spoiler area to semispan wing area S_s/S for a $0.75\frac{b}{2}$- span plain spoiler and a $0.75\frac{b}{2}$- span row of semaphore spoilers located at the 0.65c station.

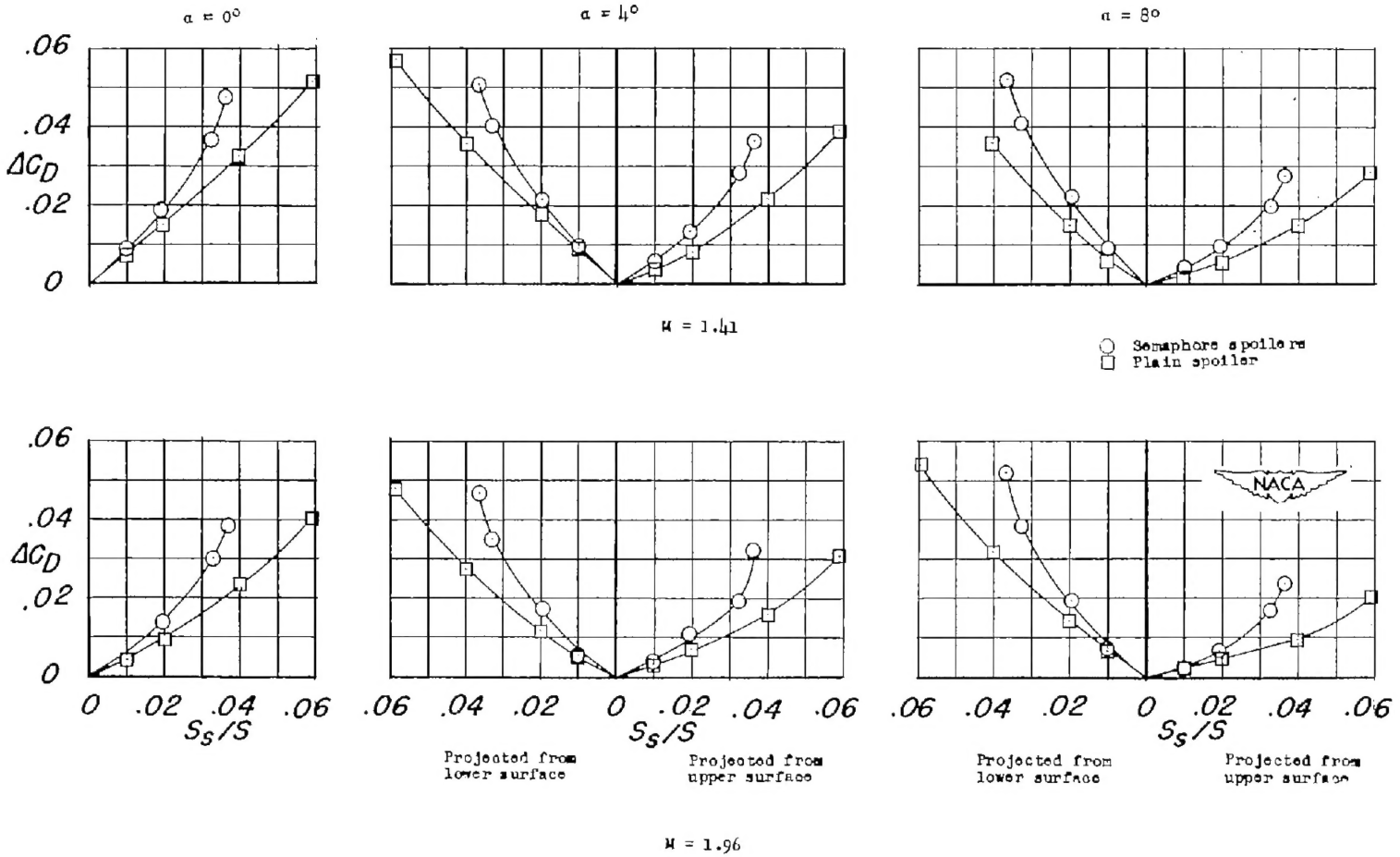

Figure 22.- Variation of incremental drag coefficient with ratio of spoiler area to semispan wing area S_s/S for a $0.75\frac{b}{2}$ - span plain spoiler and a $0.75\frac{b}{2}$ - span row of semaphore spoilers located at the 0.65c station.

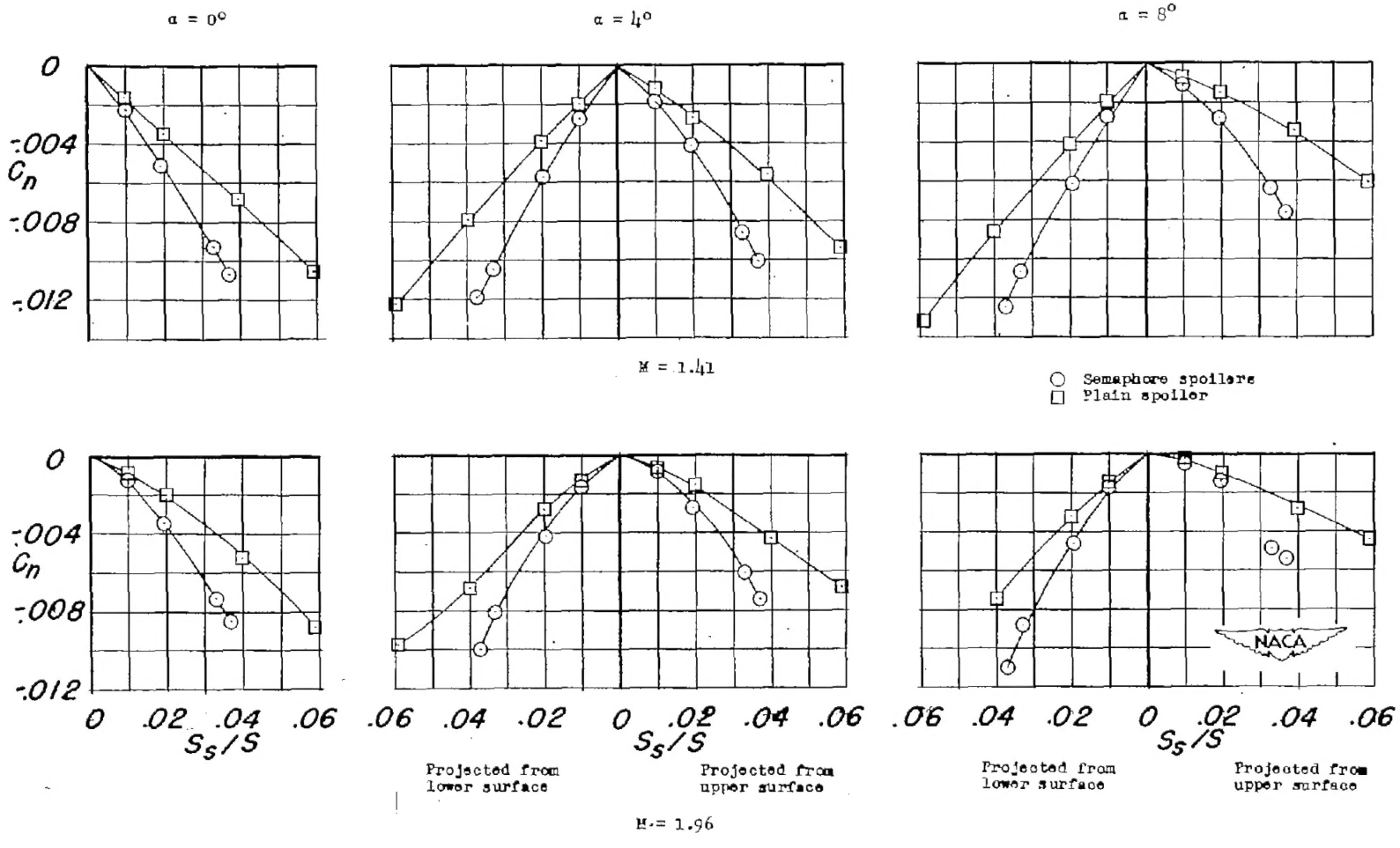

Figure 23.- Variation of yawing-moment coefficient with ratio of spoiler area to semispan wing area S_s/S for a $0.75\frac{b}{2}$ - span plain spoiler and a $0.75\frac{b}{2}$ - span row of semaphore spoilers located at the 0.65c station.